

GeSb thin films: read-write optical data storage on the subnanosecond time scale

**Albert Kim
Javier Solís
John Paul Callan
Chris Roeser
Eric Mazur**

**Ultrafast Electronics and Optoelectronics
Lake Tahoe, 11 January 2001**



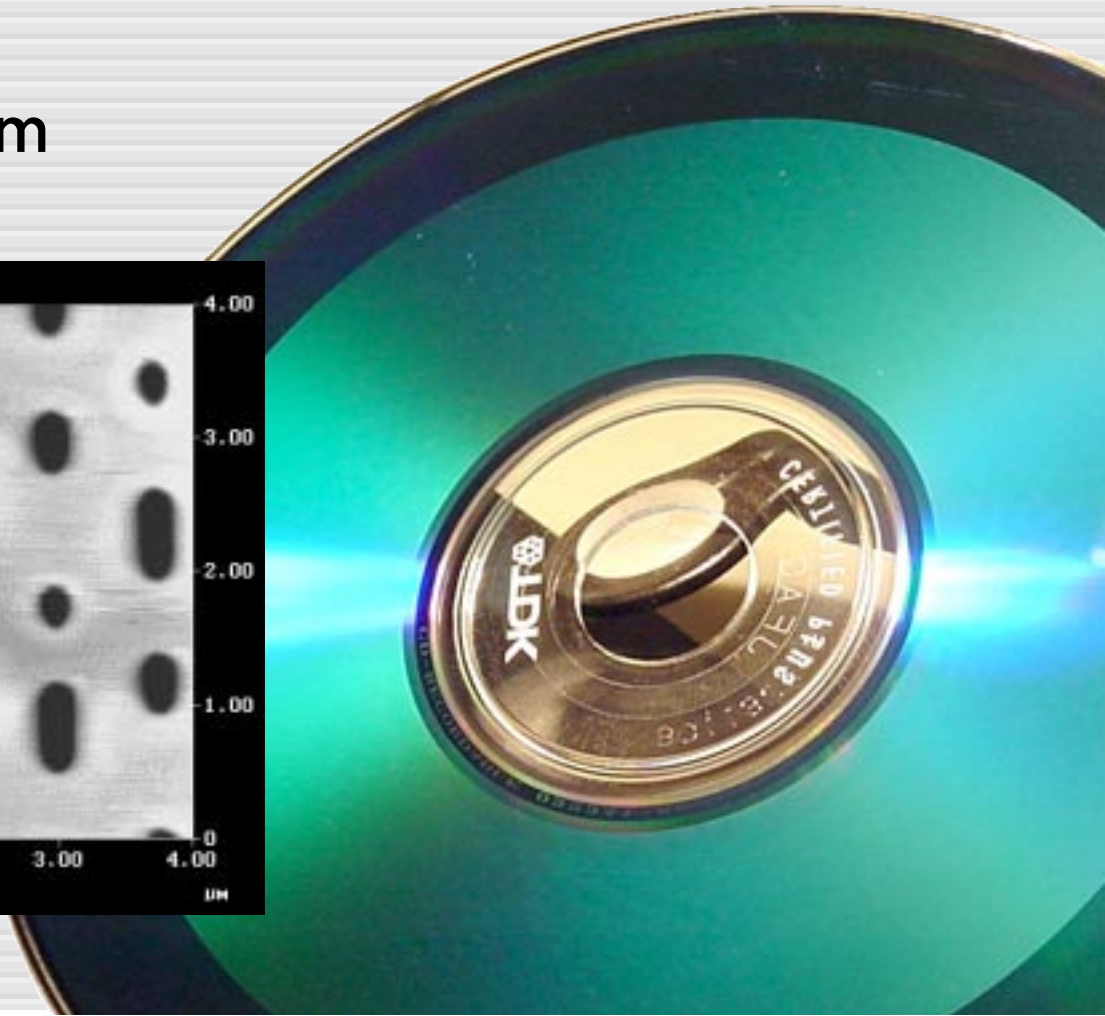
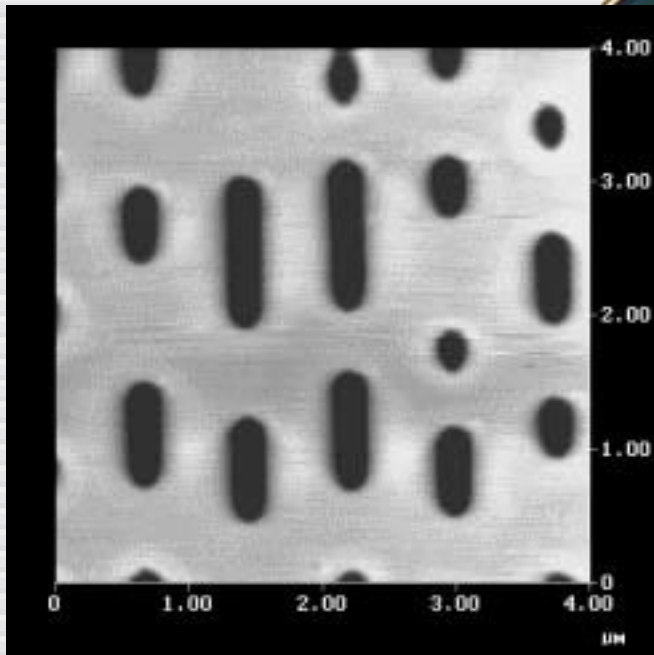
Introduction

- ▶ explosive demand for data storage
- ▶ 10^{20} bits currently
- ▶ optical data storage:
from 680 Mb to 4.7 Gb



Introduction

- ▶ bit length: $0.4 \mu\text{m}$
- ▶ track spacing: $0.74 \mu\text{m}$



Introduction

- ▶ GeSbTe phase-change rewritable medium of choice
- ▶ high fluence: amorphize (write)
- ▶ low fluence: crystallize (erase)

but... crystallization slow!



Dynamics of Ultrafast Phase Changes in Amorphous GeSb Films

K. Sokolowski-Tinten,¹ J. Solis,² J. Bialkowski,¹ J. Siegel,² C. N. Afonso,² and D. von der Linde¹

¹*Institut für Laser- und Plasmaphysik, Universität-GHS-Essen, D-45117 Essen, Germany*

²*Instituto de Optica, CSIC, C/Serrano 121, 28006 Madrid, Spain*

(Received 24 February 1998)

Time resolved imaging has been used to analyze structural transformations induced by intense 100 fs laser pulses in amorphous GeSb films. Above a threshold of 19 mJ/cm² the data show the formation of a transient nonequilibrium state of the excited material within 300 fs. The results are consistent with an electronically induced, amorphous-to-crystalline phase transition. [S0031-9007(98)07514-0]

PACS numbers: 61.80.Ba, 61.43.Dg, 68.35.Bs, 68.35.Rh

The existence of nonthermal, ultrafast phase transitions after strong femtosecond laser excitation has been demonstrated in several materials such as silicon [1-3], gallium arsenide [3-6], indium antimonide [7], and carbon [8]. It is accepted that such transitions are induced by a softening of the lattice structure due to the generation of a very high density electron-hole plasma, as first proposed by Van Vechten [9]. Most of the experimental and theoretical work [10-13] has concentrated on the solid-to-liquid transition of the above mentioned materials. The existence of an

optical microscope and provides snapshot pictures of the excited surface with 100 fs time resolution. The optical micrographs are recorded with the help of a charged coupled device detector in conjunction with a computer controlled frame-grabber. Since a single laser pulse induces permanent structural changes of the irradiated area the sample is moved between two consecutive exposures. A series of pictures, covering the entire period from the initial deposition of the laser energy (pump fluence 45 mJ/cm²) to the appearance of the final structural modifications, is shown in Fig. 1. The contrast of the images has been enhanced for reproduction purposes and thus Fig. 1 does not provide a quantitative measure of the reflectivity. Because of the large angle of the microscope (45°), the actual de-

Introduction

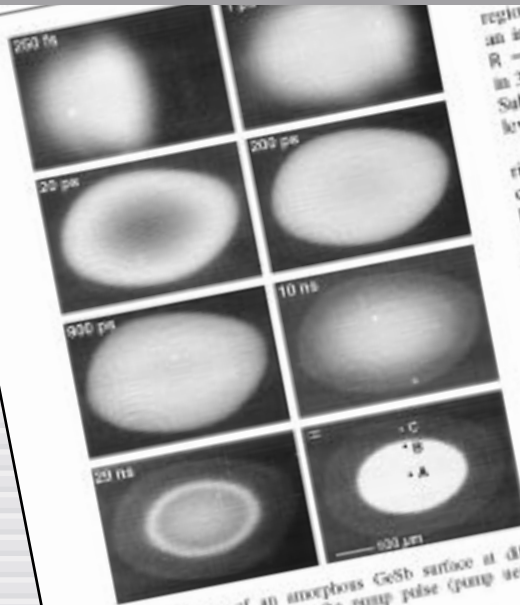


FIG. 1. Pictures of an amorphous GeSb surface at different times after exposure to the pump pulse (pump fluence 45 mJ/cm²).

The edge of the large ellipse with increased reactivity observed at $\Delta t = 200$ ps corresponds to a threshold fluence of 5 mJ/cm². The position of this edge coincides with the outer boundary of the molten transformed region ($\Delta t = 0$), which can be recognized by a slight reactivity increase compared to the initial reactivity. The permanent high reactivity phase seen in the same frame (bright ellipse) is observed only above 19 mJ/cm².

To quantitatively follow the time evolution, we have plotted in Fig. 2 the absolute reactivity (absolute error ≈ 0.005) as a function of delay time, as measured in three different locations (marked as A, B, and C in the frame $\Delta t = 0$ in Fig. 1). Trace A represents the time dependence at maximum fluence (45 mJ/cm²), traces B and C correspond to fluences of 20 and 12 mJ/cm², respectively, slightly above and well below the threshold for the appearance of the molten high reactivity phase. At the highest fluence (curve A) the reactivity increases to a maximum value of 0.71 in less than a picosecond. Then it decreases slowly towards a minimum at $\Delta t \approx 200$ ps and rises again reaching values of 0.68 and 0.69 in about 200 ps and 2 ns, respectively. The reactivity remains then nearly constant up to about 10 ns. A second reactivity minimum is observed at $\Delta t \approx 30$ ns, followed by a molten increase to a stationary value of 0.71. Trace B shows a similar

region of... an initial subpicosecond... $R = 0.71$. Instead, the reactivity... in 30 ps and stays then constant up to about 100 ps. Subsequently, it starts to decrease reaching a stationary level of $R = 0.59$ after 30 ns.

The reactivity of the liquid and crystalline phase of Sb-rich GeSb is known at 633 nm [15,19] and nearly identical to that of pure Sb (*l*-Sb: $R = 0.67$, *c*-Sb: $R = 0.71$, [20]). The reactivity of the amorphous phase is significantly lower, $R = 0.57$ [0.58, slightly dependent on composition and state of structural relaxation [21]. Thus the observation of a nearly constant reactivity level with $R = 0.69$ in the ps to ns time domain for fluences above 5 mJ/cm² can be attributed to melting of the material over a thickness larger than the penetration depth of the probe pulse radiation. The molten reactivity of 0.71 observed above 19 mJ/cm² (traces A and B) indicates the formation of crystalline material upon solidification, while between 5 and 19 mJ/cm² the resolved material is amorphous (trace C). The slight difference between initial and molten reactivity of the amorphous material is amorphous state of structural relaxation [21]. The nanosecond behavior of the reactivity above the crystallization threshold $F_{cr} = 19$ mJ/cm² is quite similar to what has been measured on GeSb films irradiated with ns and ps pulses [15,19]. In particular the reactivity minimum observed in the tens of ns time scale in traces A and B is related to bulk nucleation of amorphous material within the molten

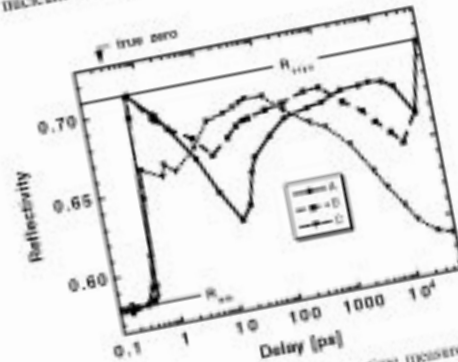


FIG. 2. Reactivity as a function of delay time measured at three different locations (marked as A, B, and C in the last frame of Fig. 1), corresponding to excitation fluences of 45, 20, and 12 mJ/cm², respectively. The rightmost data point of each curve represents the molten reactivity ($\Delta t = 0$). Note the logarithmic time axis, the true zero delay (see text) is marked by an arrow.

Introduction

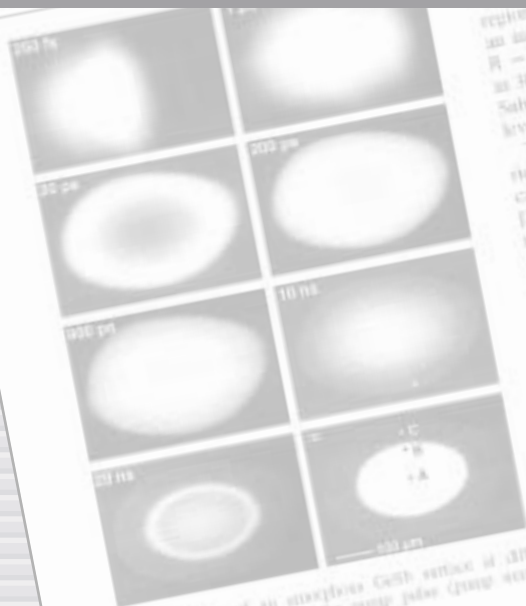


FIG. 1. Pictures of an amorphous GeSb surface at different times after exposure to the pump pulse (pump energy: 45 mJ/cm²).

The edge of the large ellipse with increased reactivity observed at $\Delta t = 200$ ps corresponds to a threshold reactivity of 5 mJ/cm². The position of this edge coincides with the outer boundary of the molten transformed region ($\Delta t = 0$) which can be recognized by a slight reactivity increase compared to the initial reactivity. The perimeter high reactivity phase seen in the same frame (bright ellipse) is observed only above 19 mJ/cm².

To quantitatively follow the time evolution, we have plotted in Fig. 2 the absolute reactivity (absolute error ≈ 0.005) as a function of delay time, as measured in three different locations (marked as A, B, and C in the three different locations marked as A, B, and C in the dependence on maximum reactivity of 20 and 12 mJ/cm², respectively, slightly above and well below the threshold for the appearance of the molten high reactivity phase. At the highest reactivity (curve A) the reactivity increases to a maximum value of 0.71 in less than a picosecond. Then it decreases slowly towards a minimum at $\Delta t = 20$ ps and rises again reaching values of 0.68 and 0.69 in about 200 ps and 2 ns, respectively. The reactivity remains then nearly constant up to about 30 ns, followed by a molten increase to a stationary value of 0.71. Trace B shows a similar

region of the surface. The reactivity starts at an initial value of 0.69. It increases to a maximum of 0.71 in about 100 fs. It then remains constant up to about 100 ps. Subsequently, it starts to decrease reaching a stationary level of $R = 0.59$ after 30 ns.

The reactivity of the liquid and crystalline phase of Sh-rich GeSb is known at 633 nm [15,19] and nearly identical to that of pure Sh ($R = 0.67$, c-Sh: $R = 0.71$, [20]). The reactivity of the amorphous phase is significantly lower, $R = 0.57$ (0.58, slightly dependent on composition and state of structural reactivity level with the observation of a nearly constant reactivity level with $R = 0.69$ in the ps to ns time domain for reactivities above 5 mJ/cm² can be attributed to melting of the material over a thickness larger than the penetration depth of the probe pulse radiation. The molten reactivity of 0.71 observed above 19 mJ/cm² (traces A and B) indicates the formation of crystalline material upon solidification, while between 5 and 19 mJ/cm² the reactivity of 0.71 observed (trace C). The slight difference between initial and molten reactivity of the amorphous is related to differences in its state of structural reactivity [21]. The nanosecond behavior of the reactivity above the crystallization threshold $F_{th} = 19$ mJ/cm² is quite similar to what has been measured in GeSb films irradiated with ns and ps pulses in the lens of ns time scale in traces A and B is related to bulk indication of amorphous material within the molten

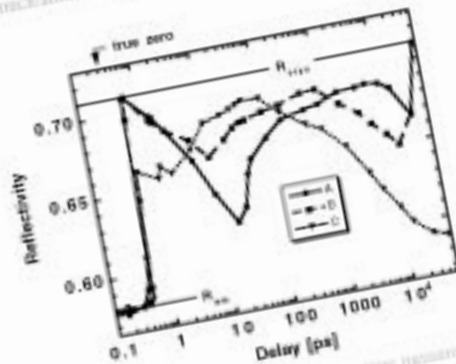
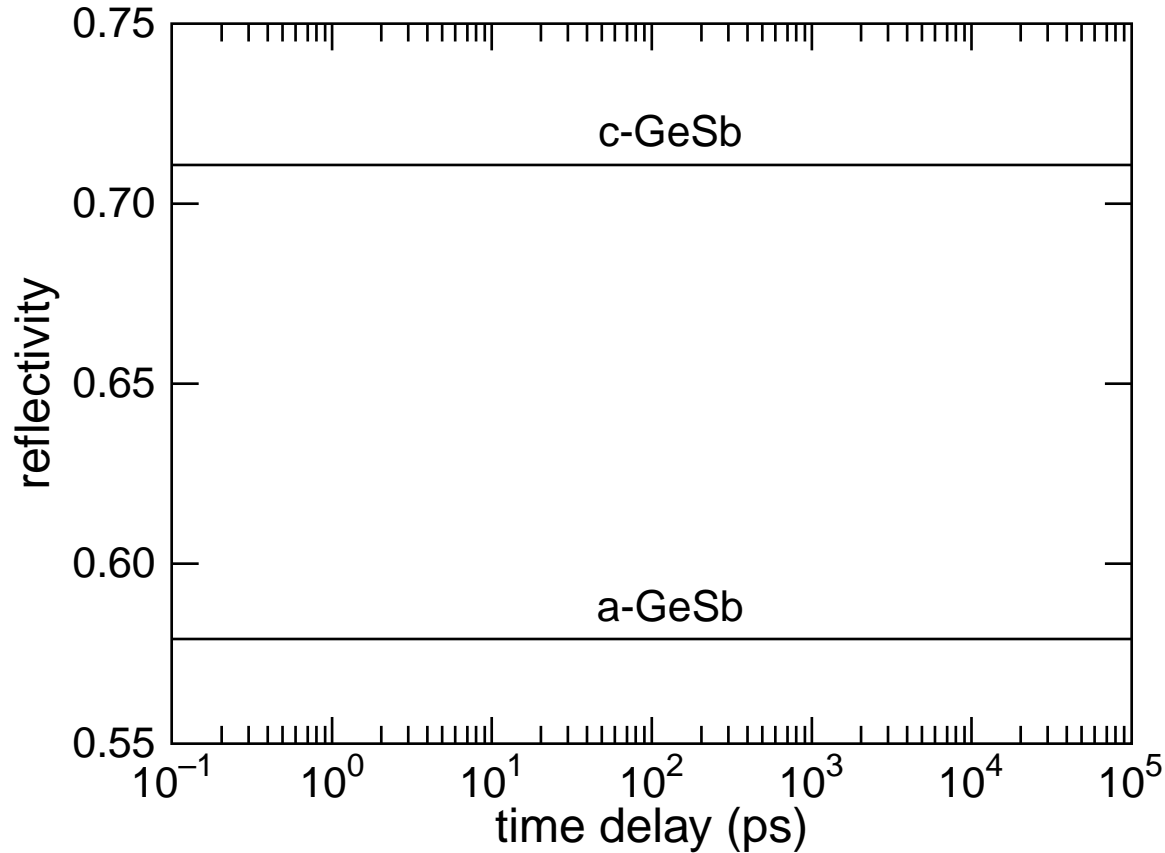
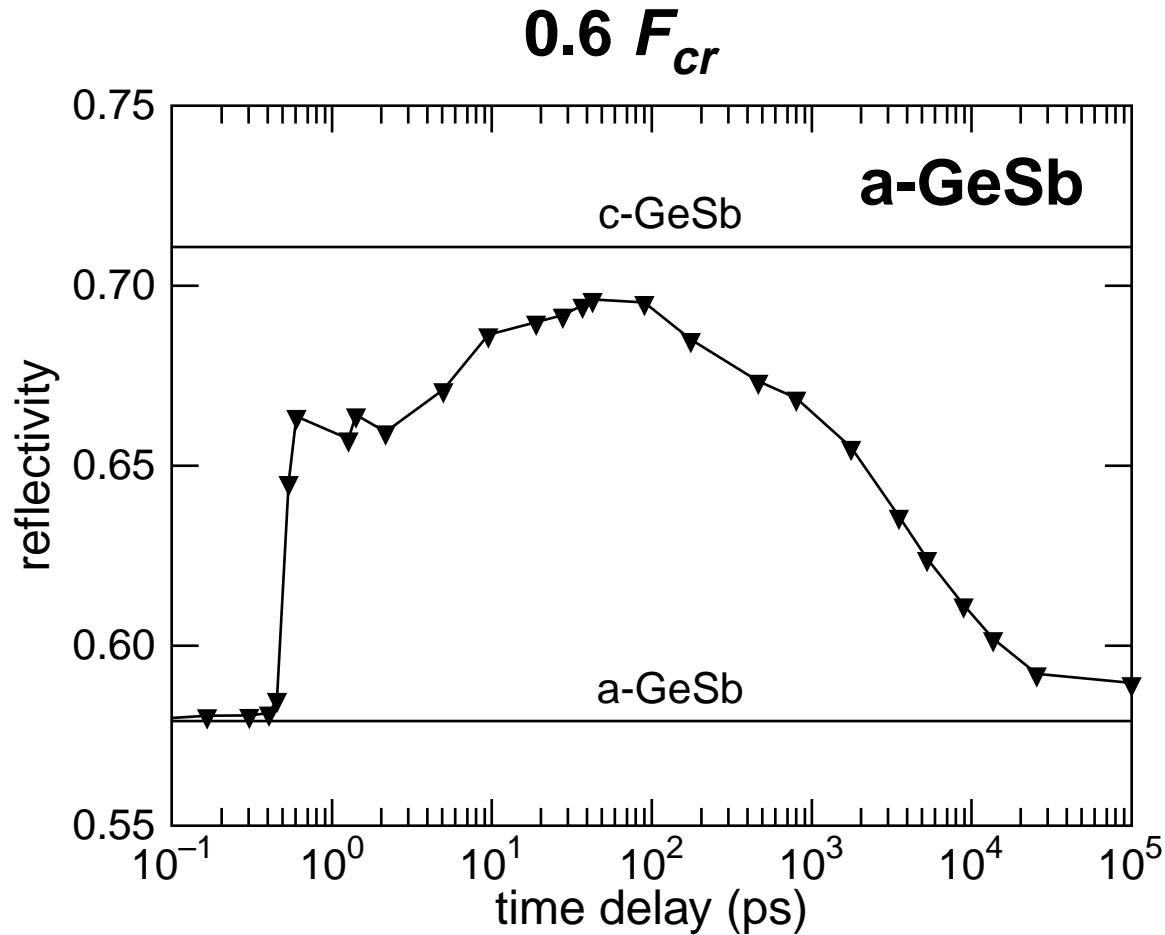


FIG. 2. Reflectivity as a function of delay time measured at three different locations (marked as A, B, and C in the text) of 45, 20, and 12 mJ/cm², respectively. The vertical dashed line of each curve represents the molten reactivity ($\Delta t = 0$). Near the logarithmic time axis, the true zero delay (see text) is marked by an arrow.

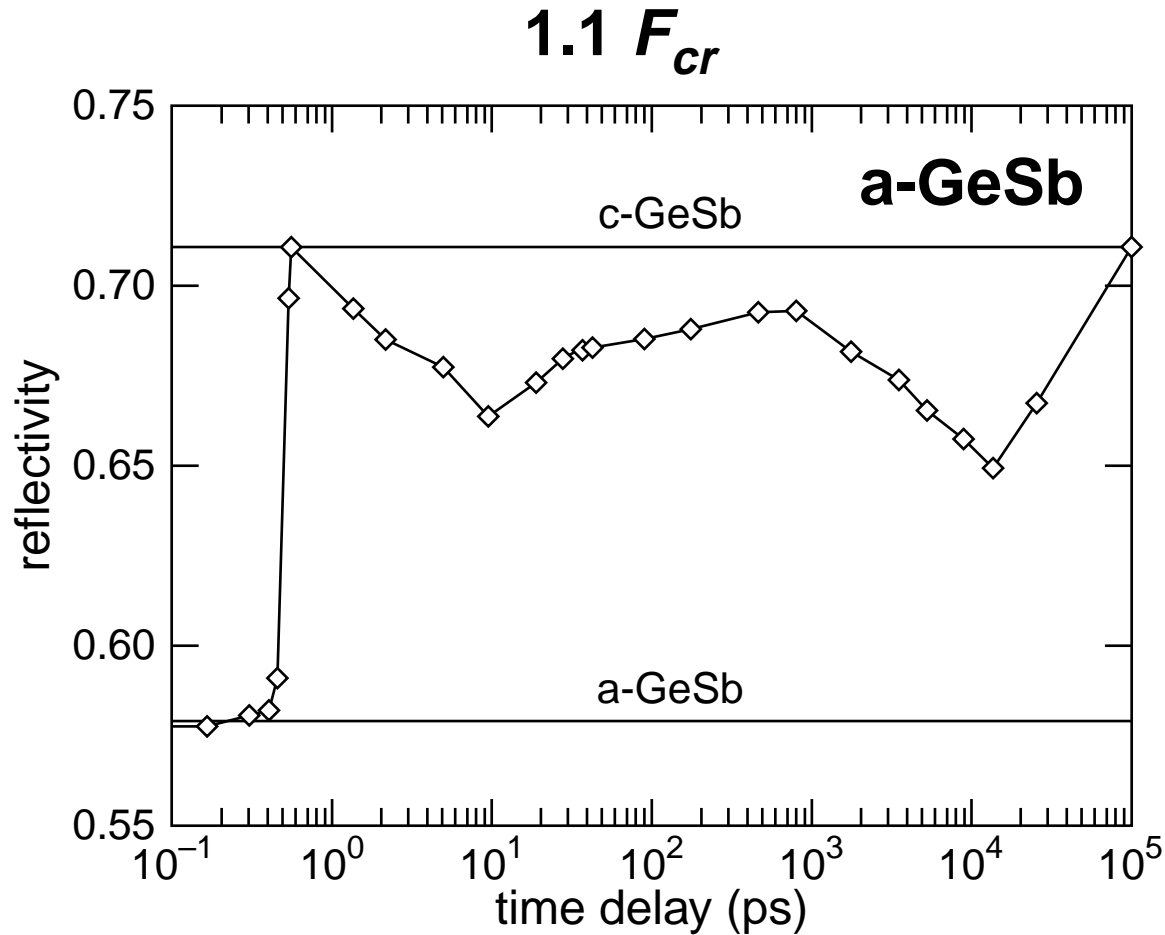
Introduction



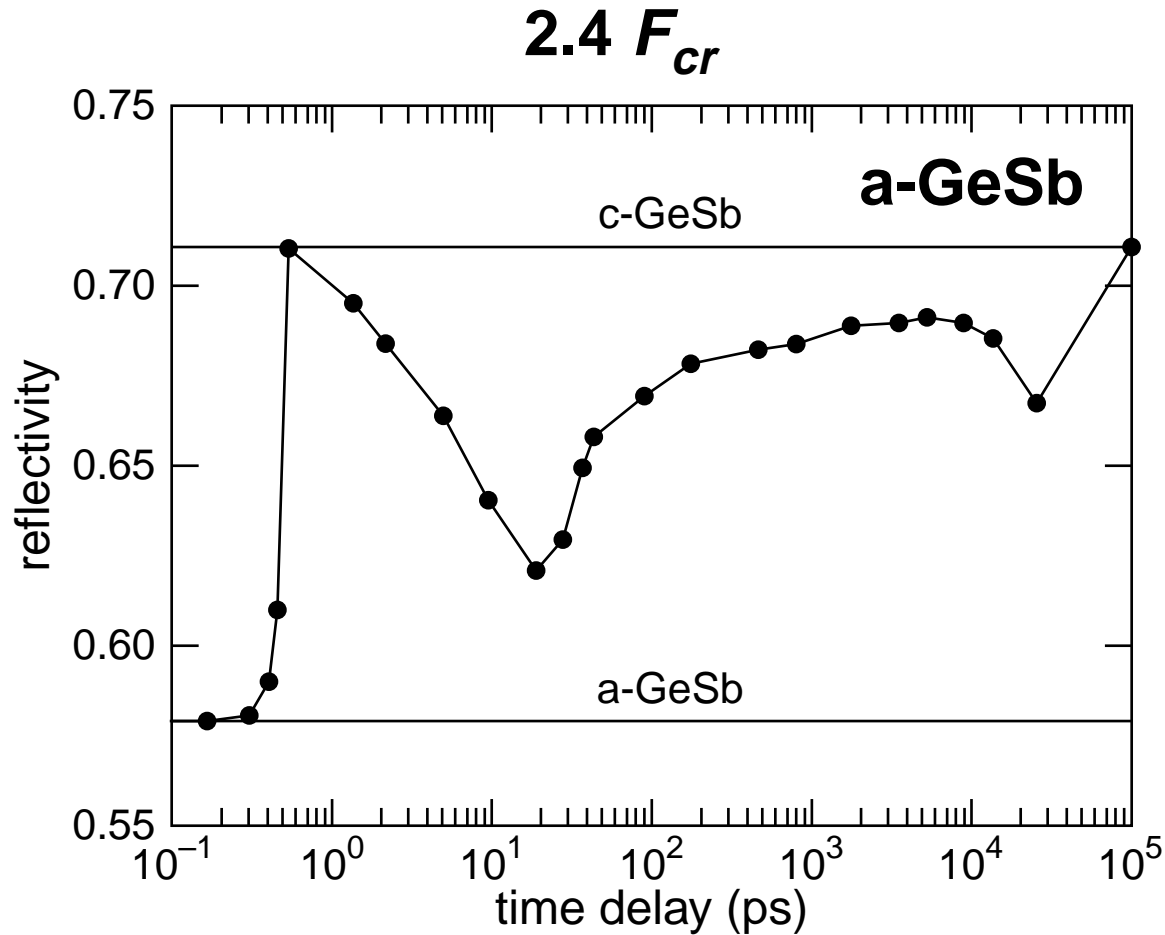
Introduction



Introduction

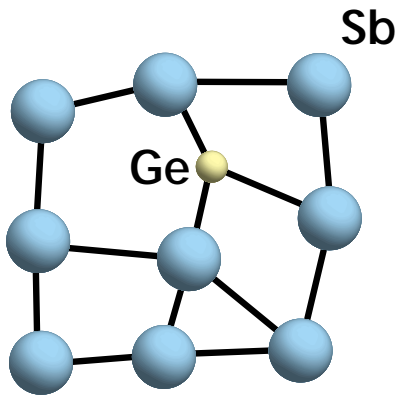


Introduction



Introduction

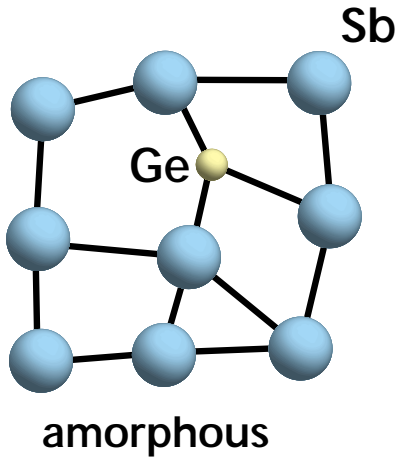
structure



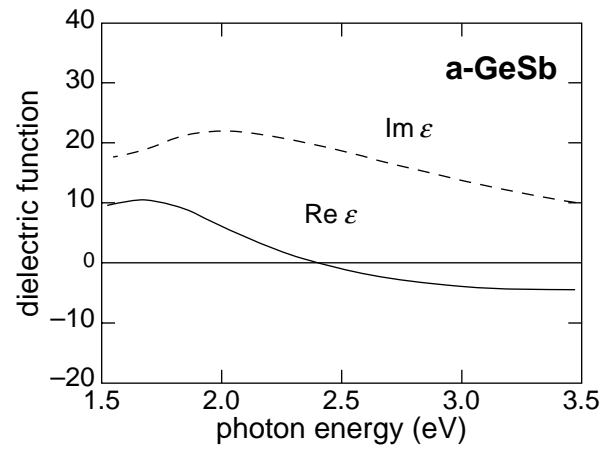
amorphous

Introduction

structure

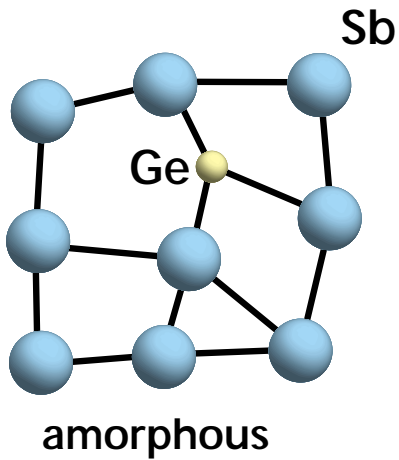


dielectric function

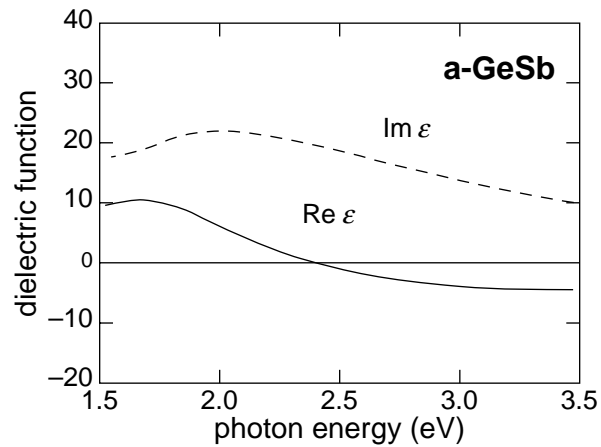


Introduction

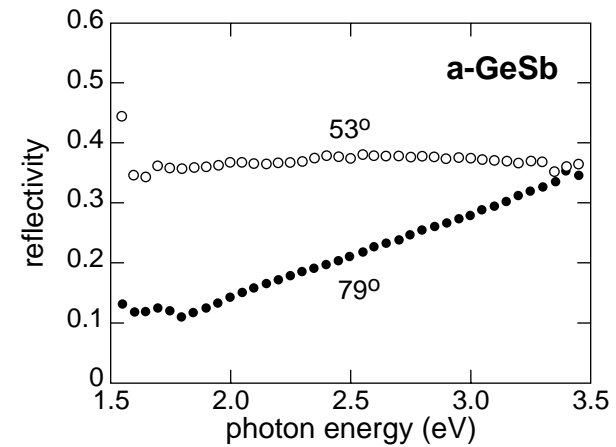
structure



dielectric function

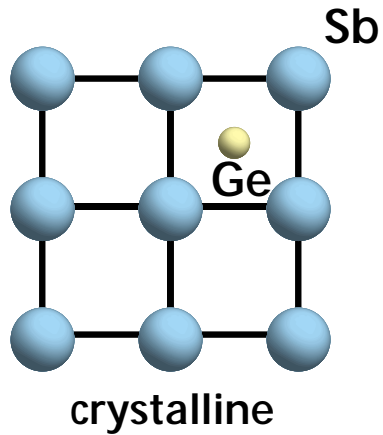


reflectivity

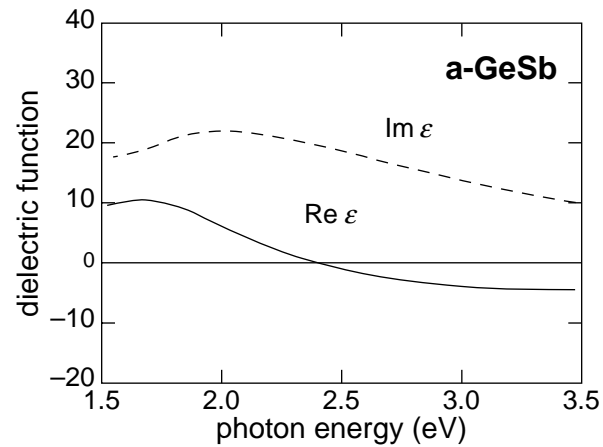


Introduction

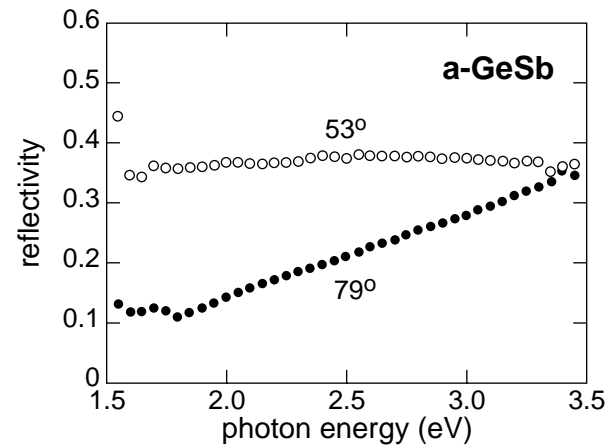
structure



dielectric function

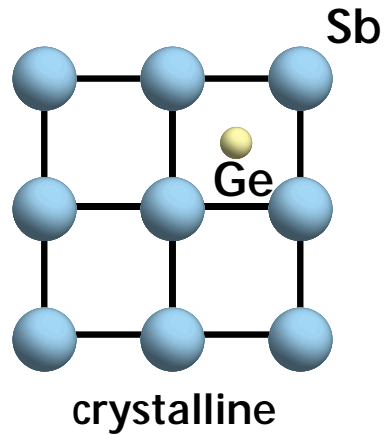


reflectivity

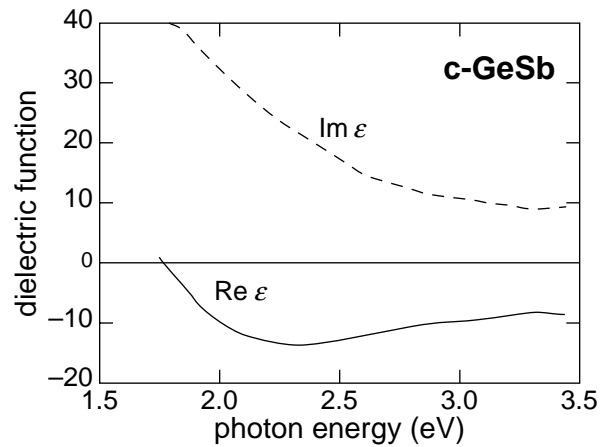


Introduction

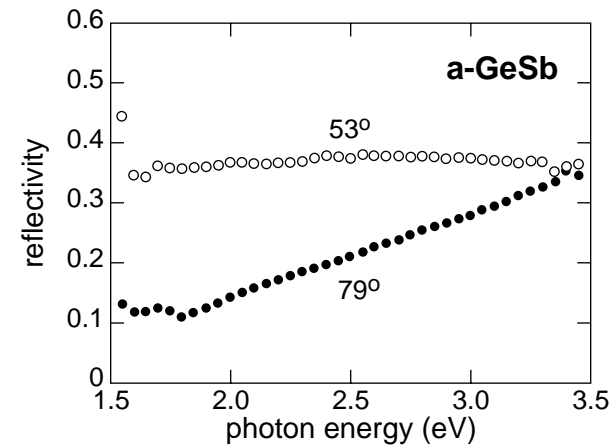
structure



dielectric function

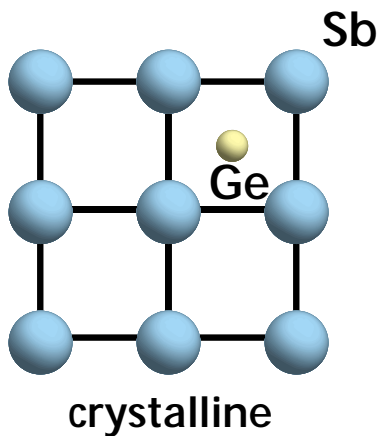


reflectivity

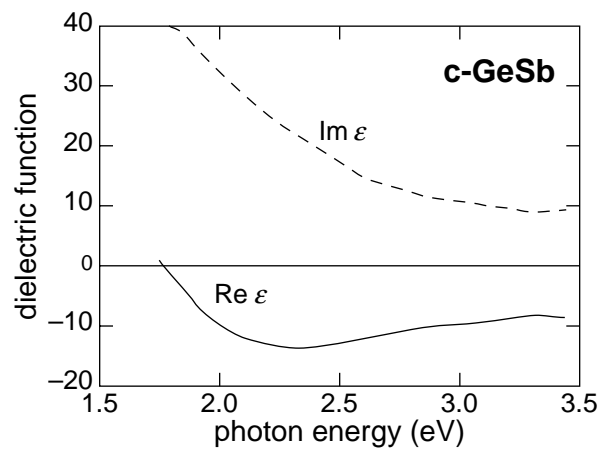


Introduction

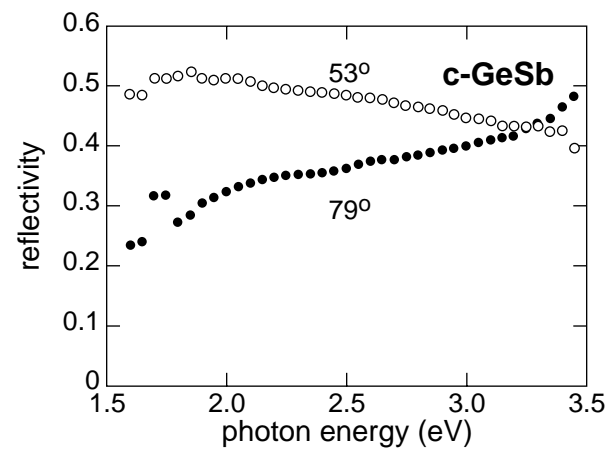
structure



dielectric function

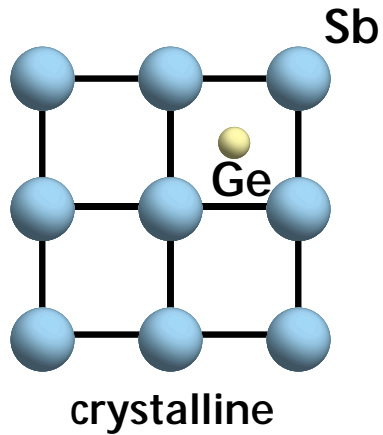


reflectivity

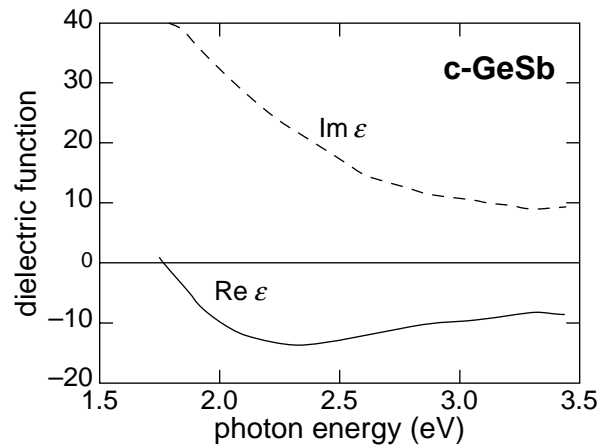


Introduction

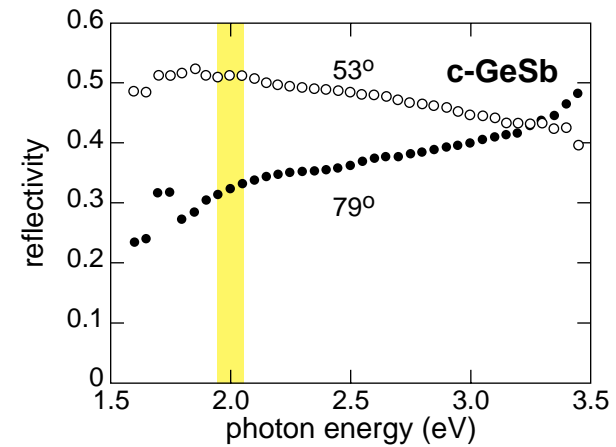
structure



dielectric function

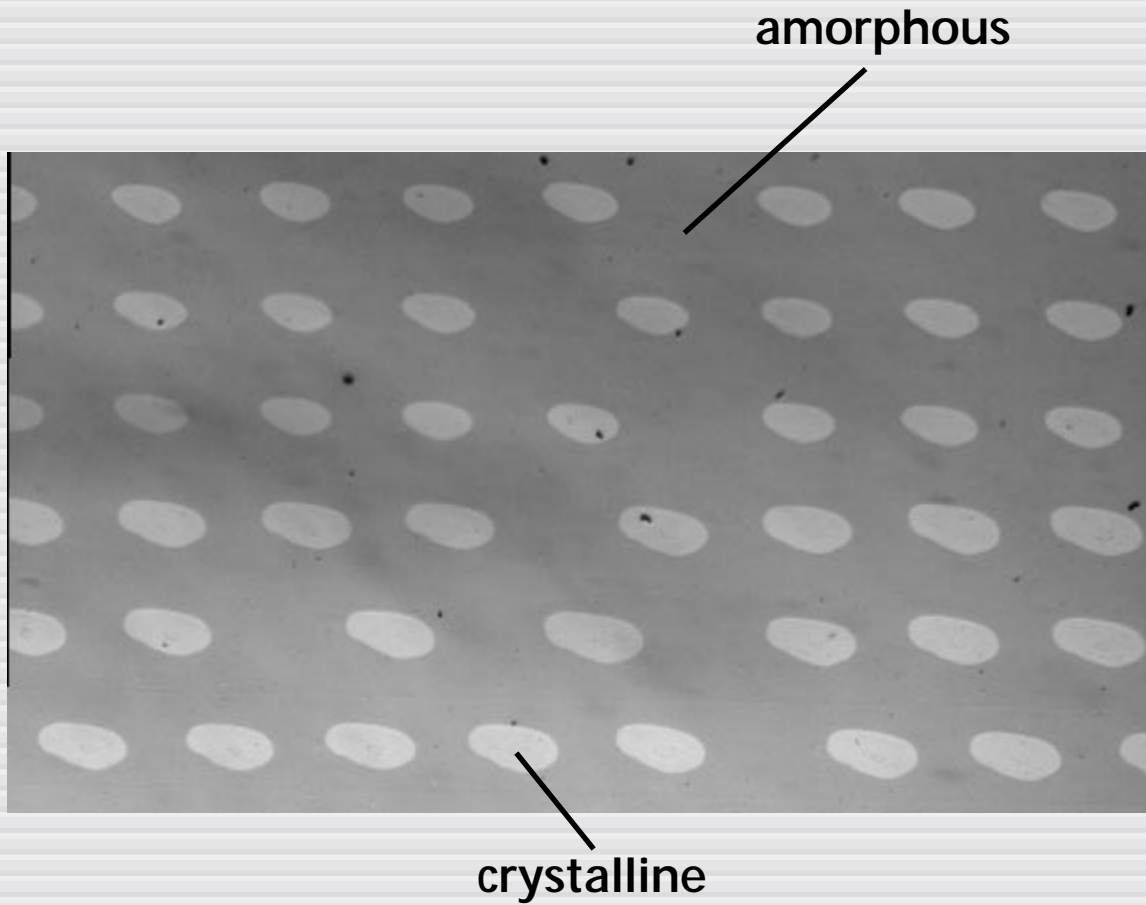


reflectivity

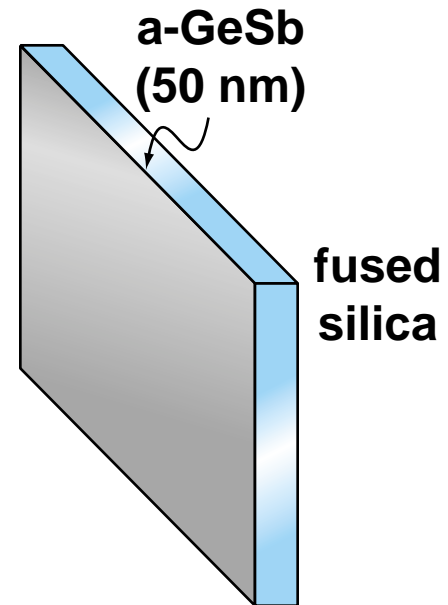


Introduction

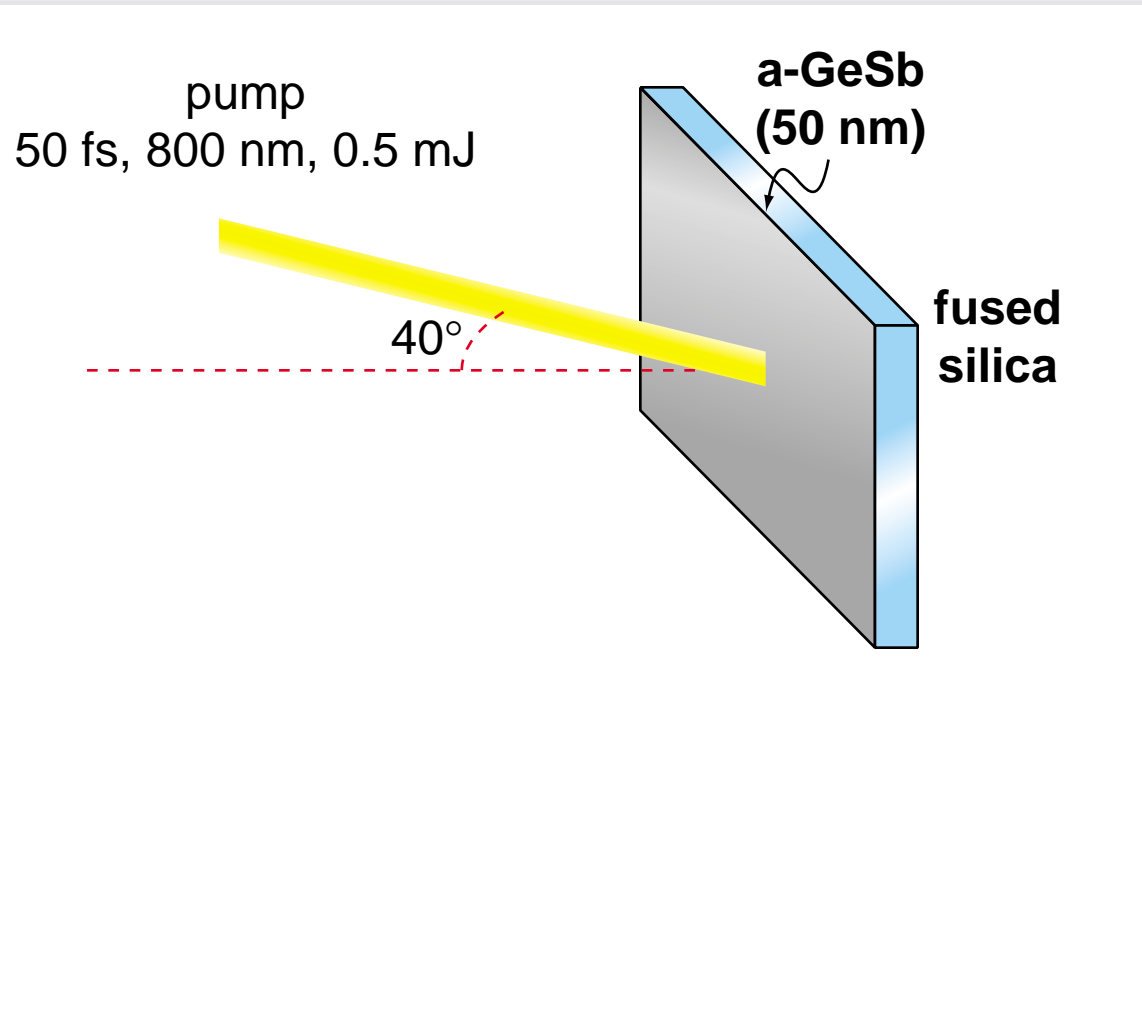
reflectivity change



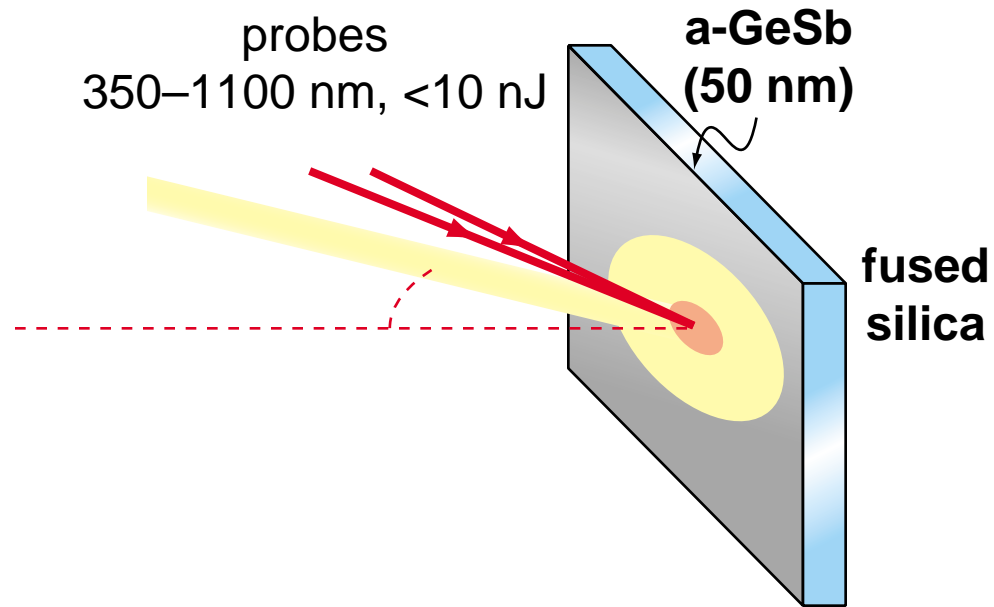
Method



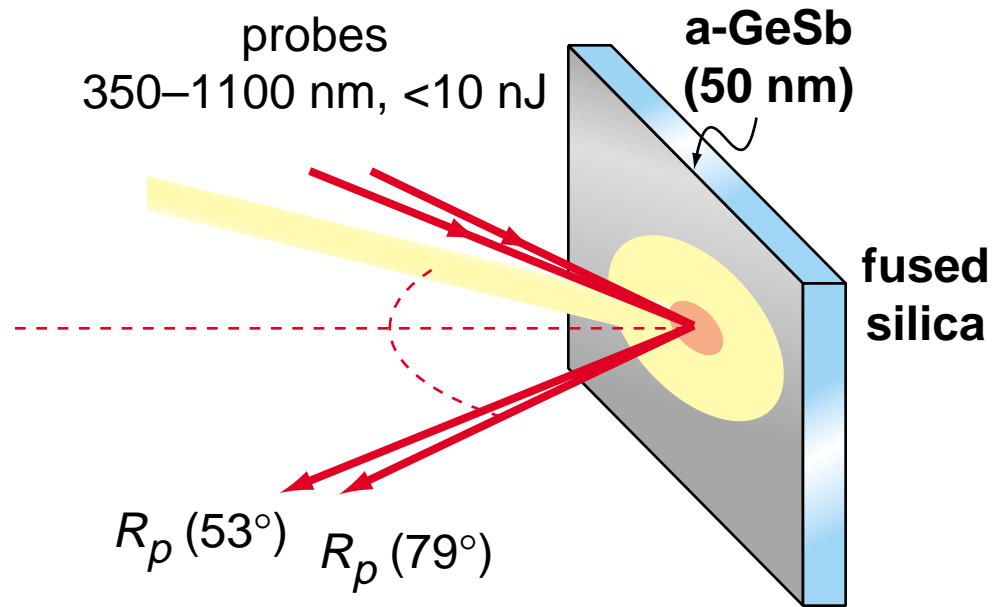
Method



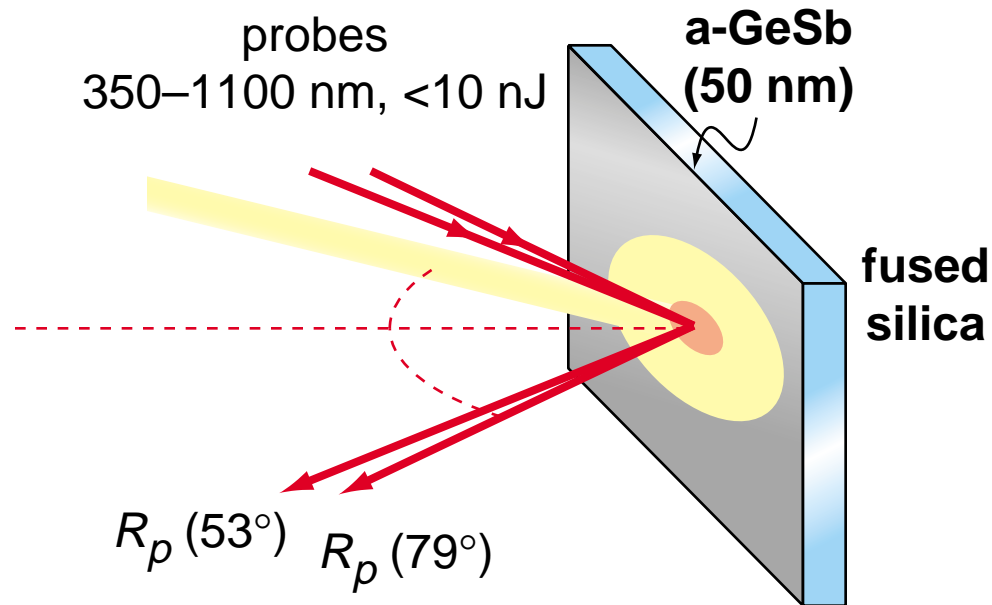
Method



Method

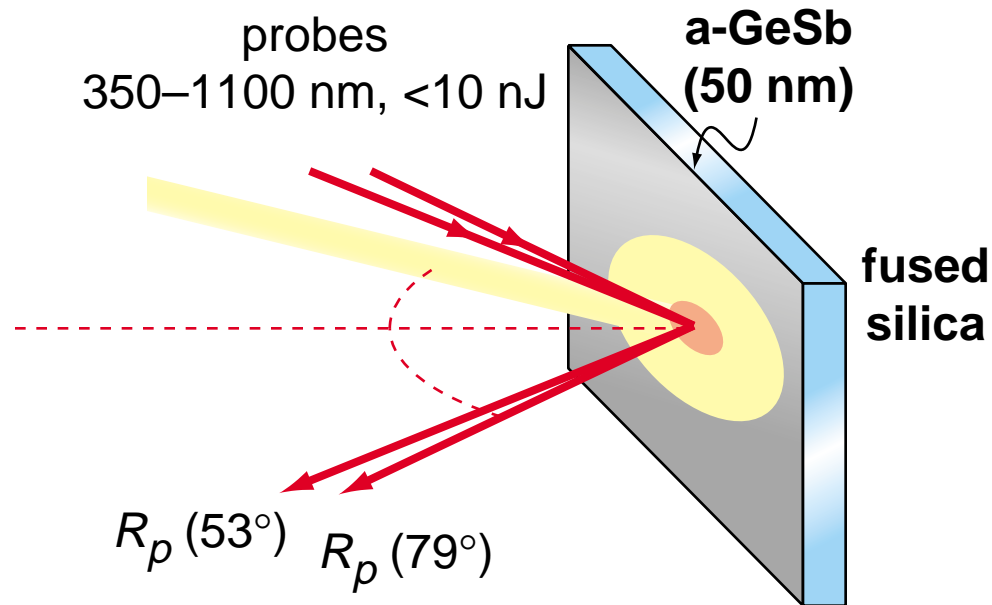


Method



Fresnel
equations

Method

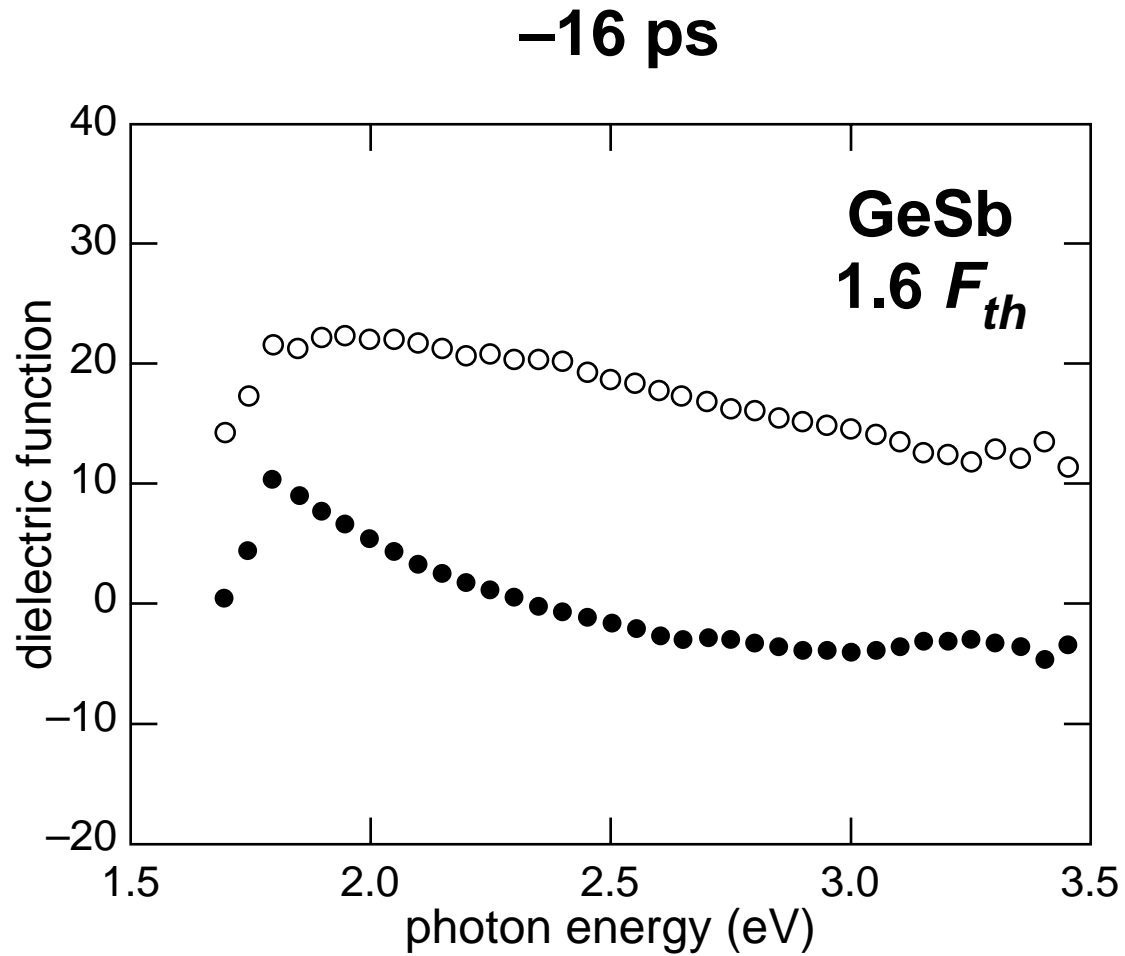


↓
Fresnel
equations



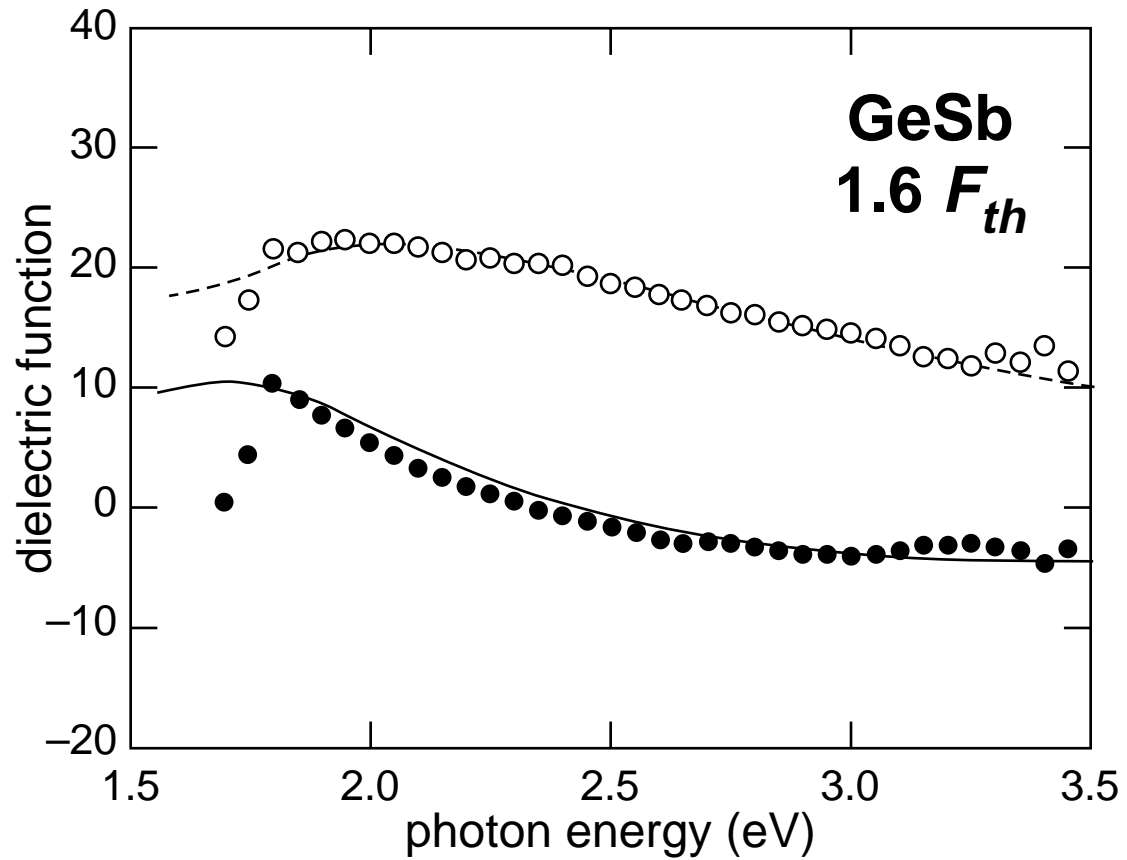
$\text{Re } \epsilon(\omega)$
 $\text{Im } \epsilon(\omega)$

Results

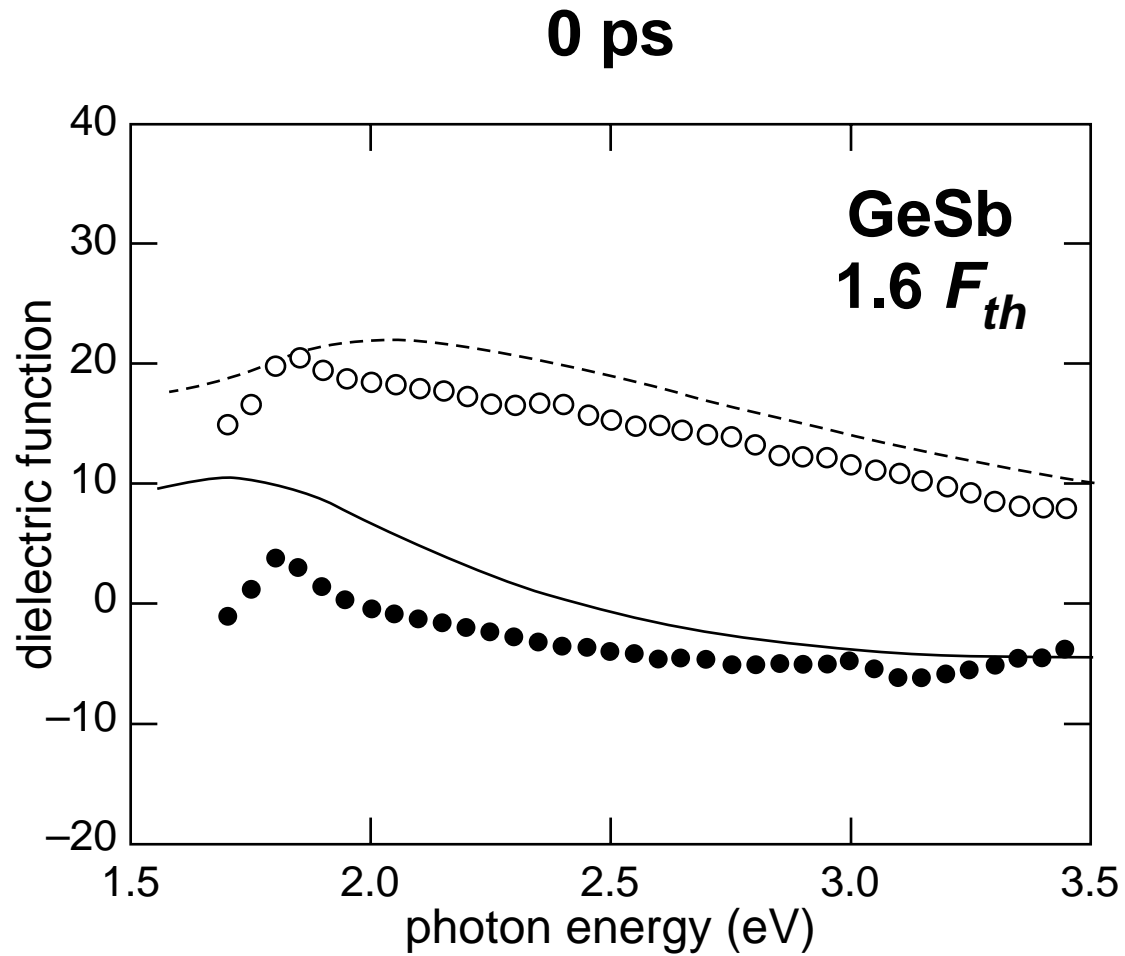


Results

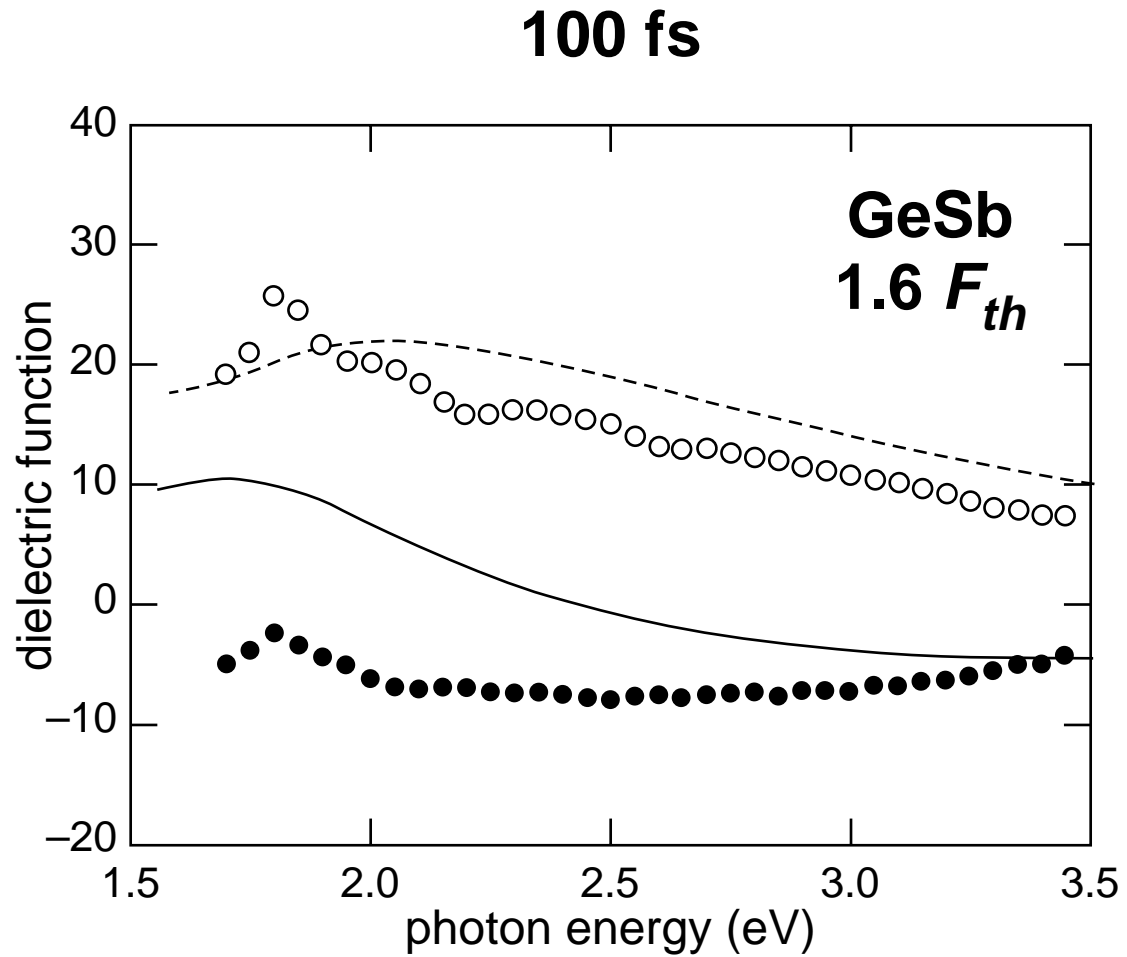
-16 ps



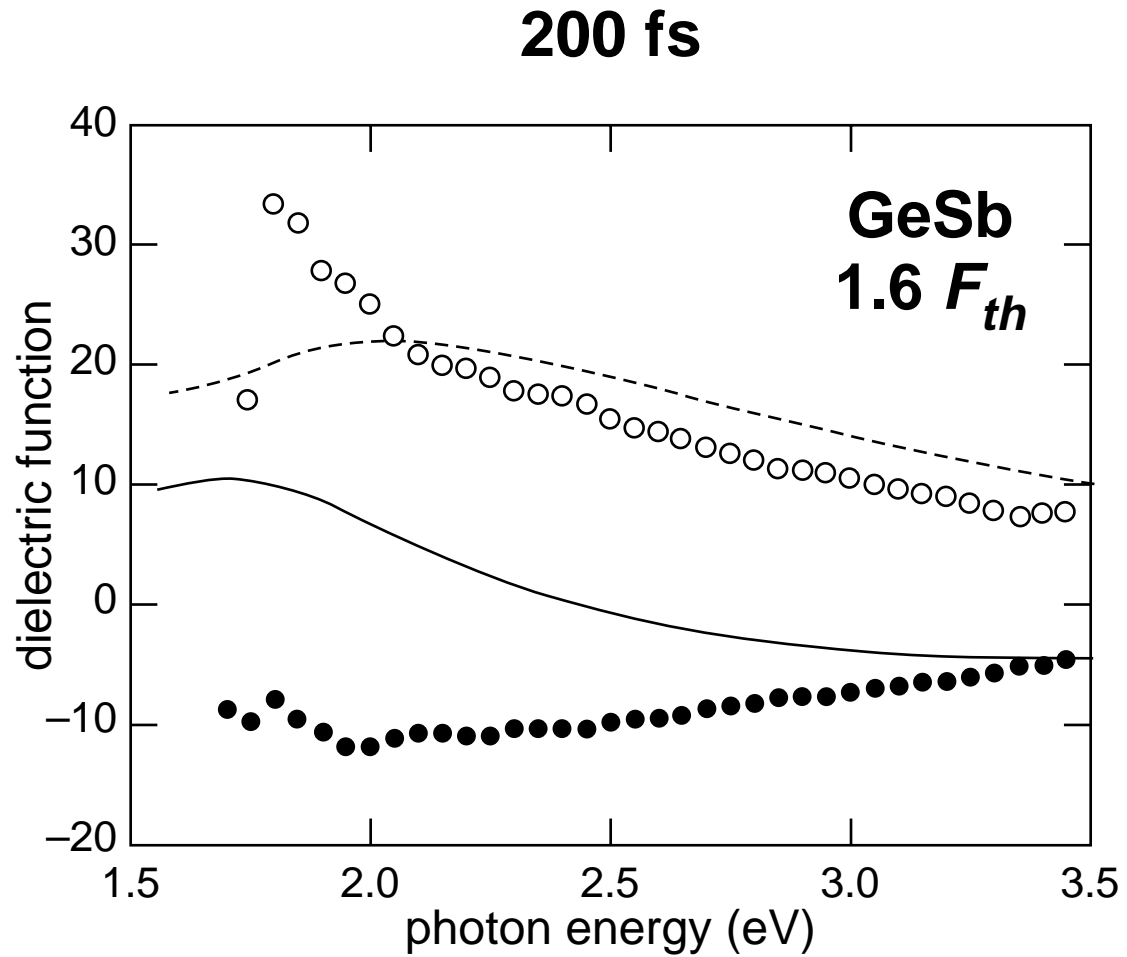
Results



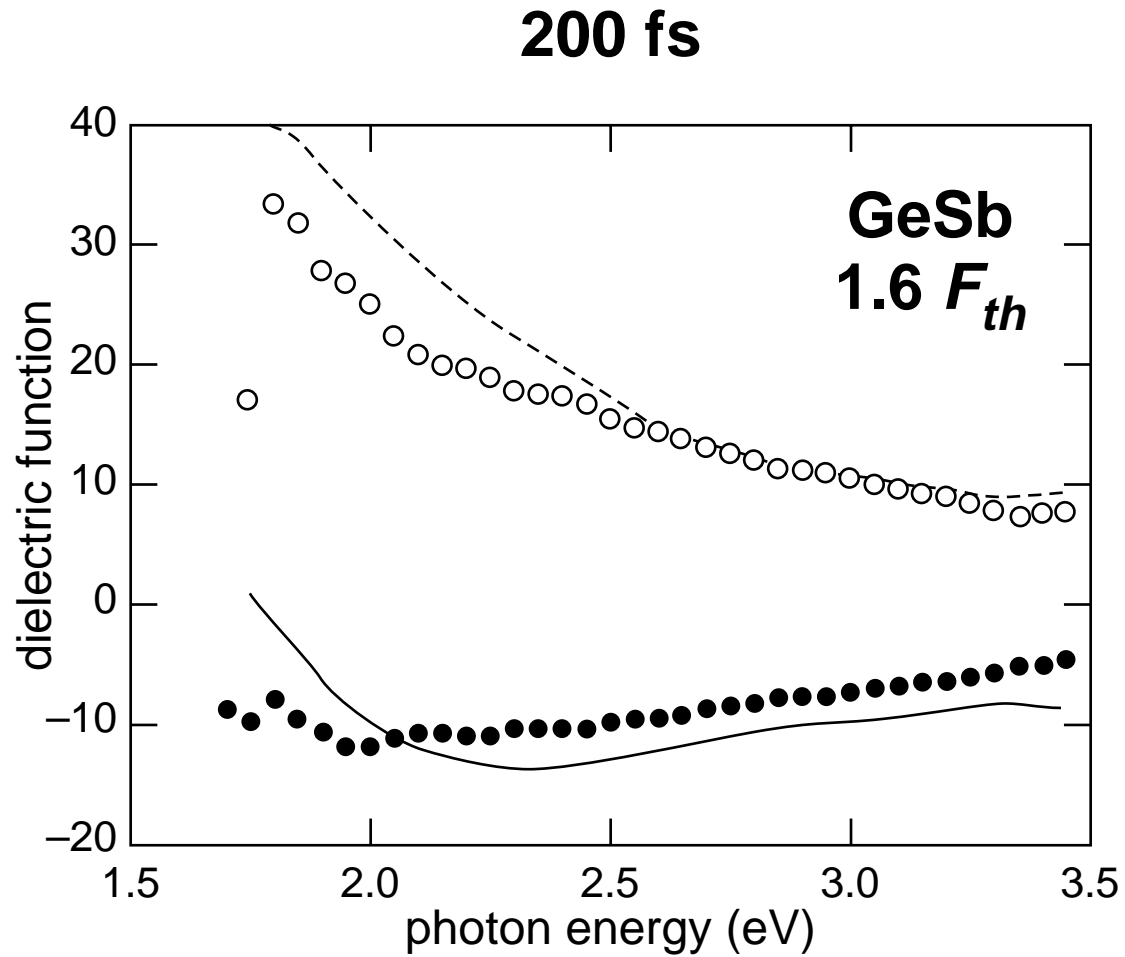
Results



Results

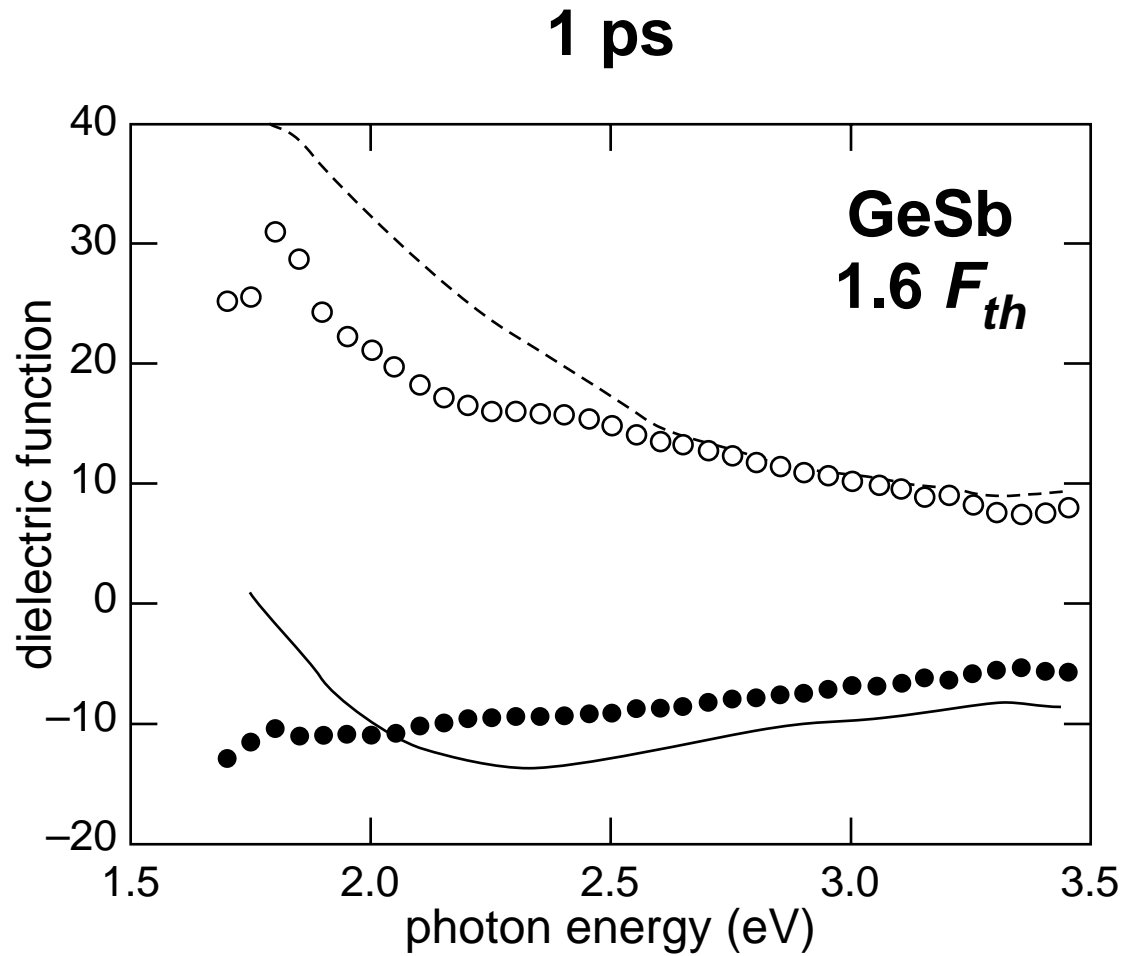


Results



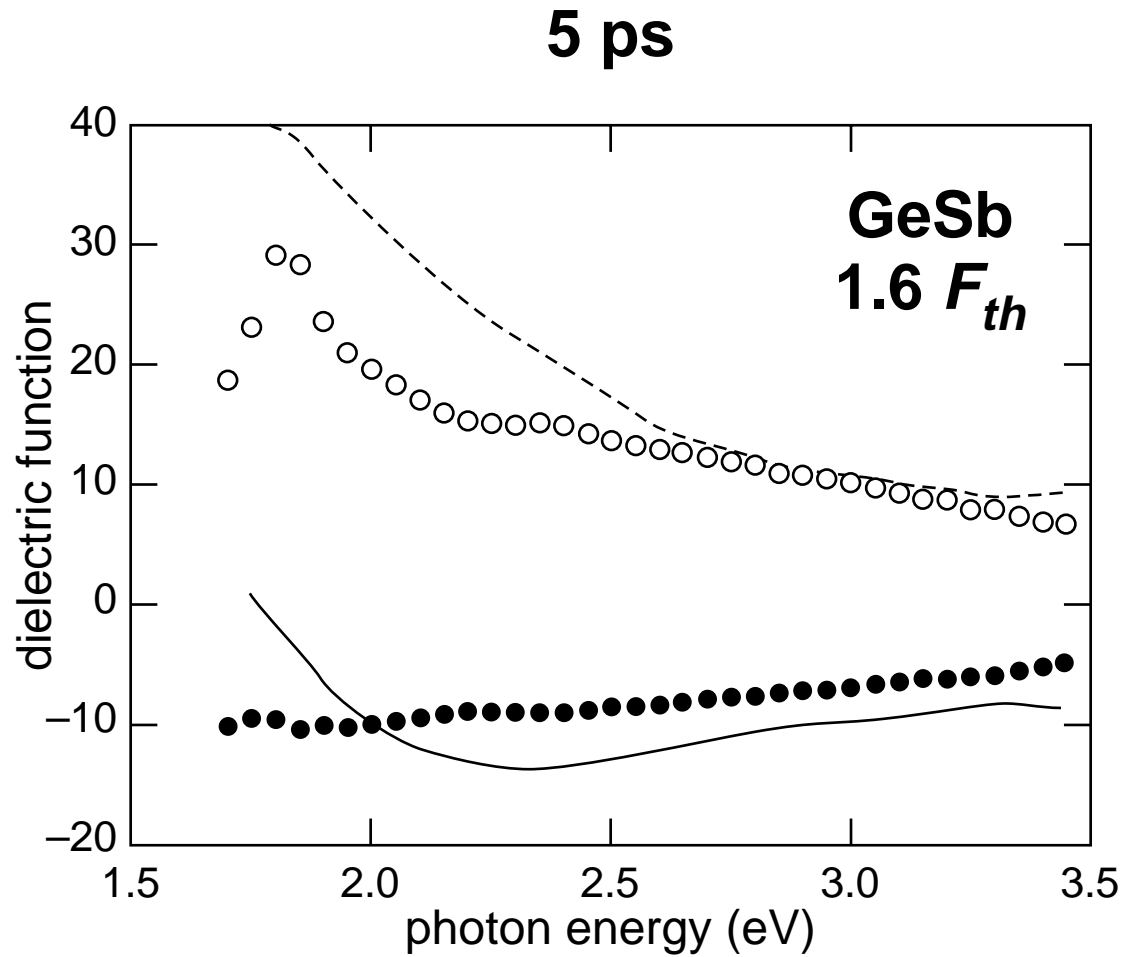
not crystalline

Results



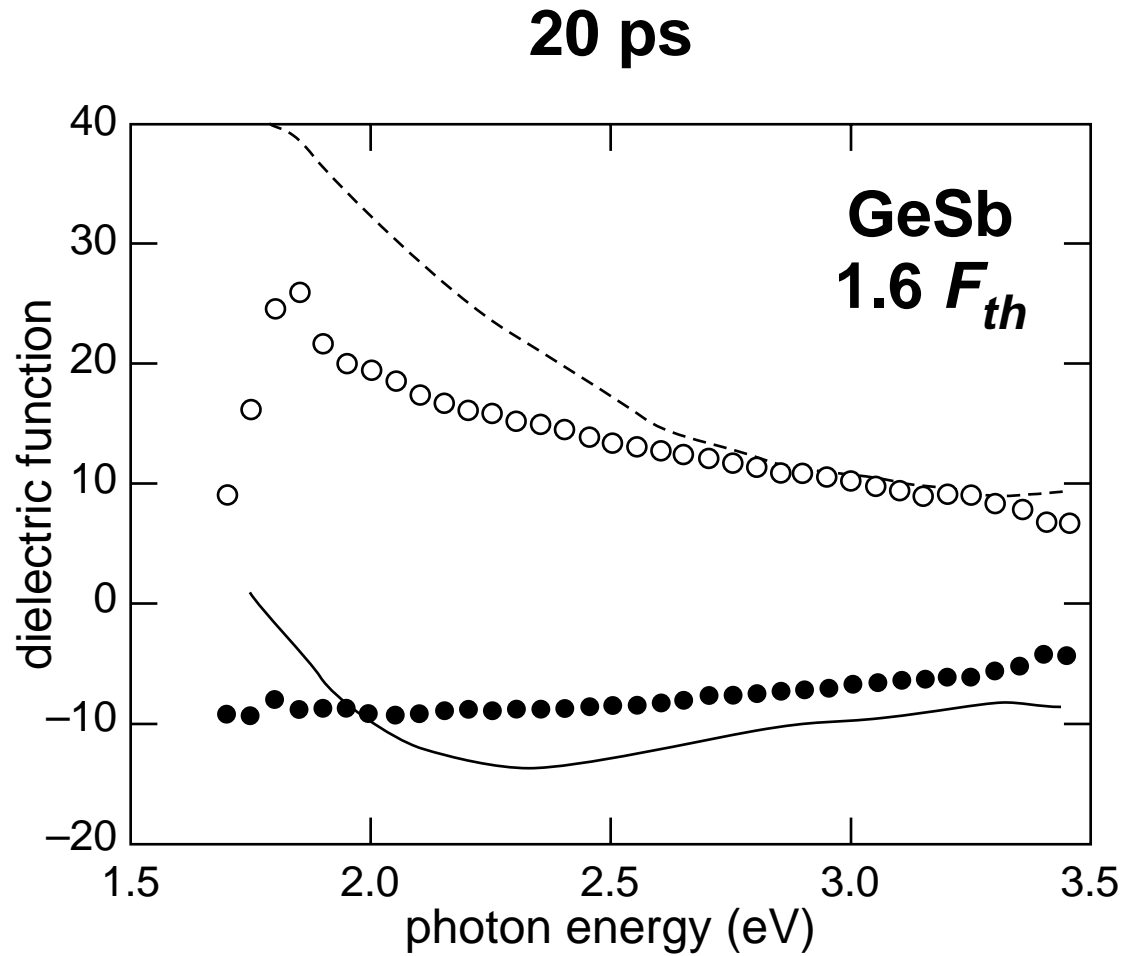
not crystalline

Results



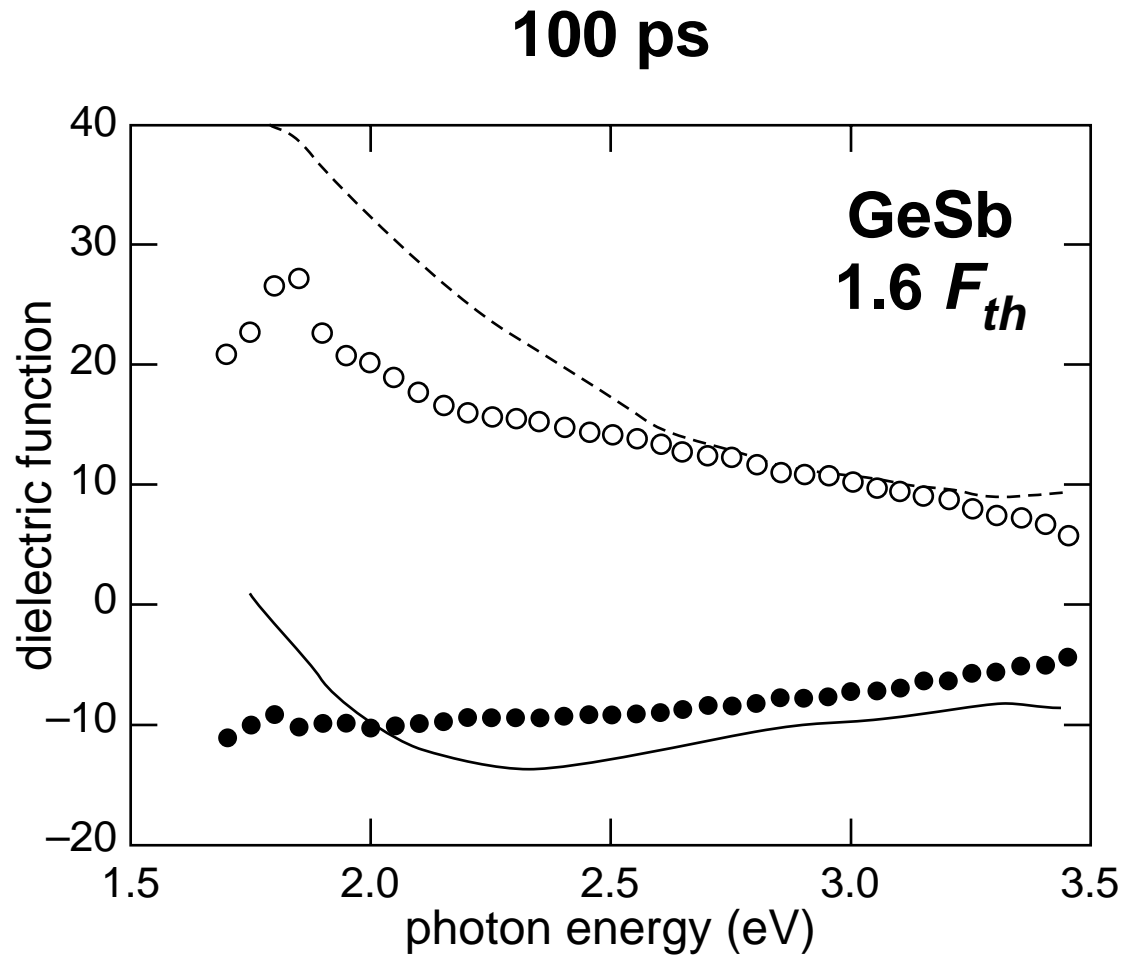
not crystalline

Results



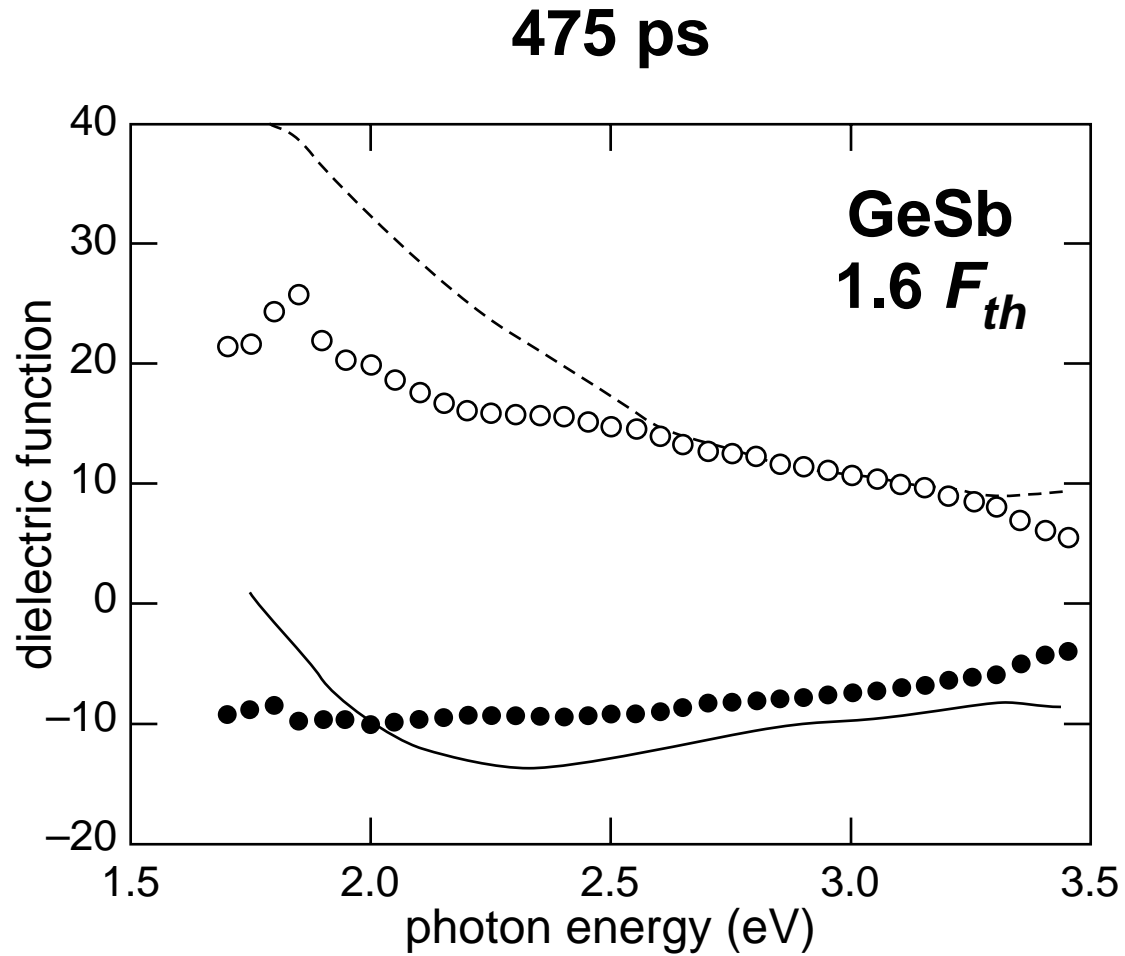
not crystalline

Results



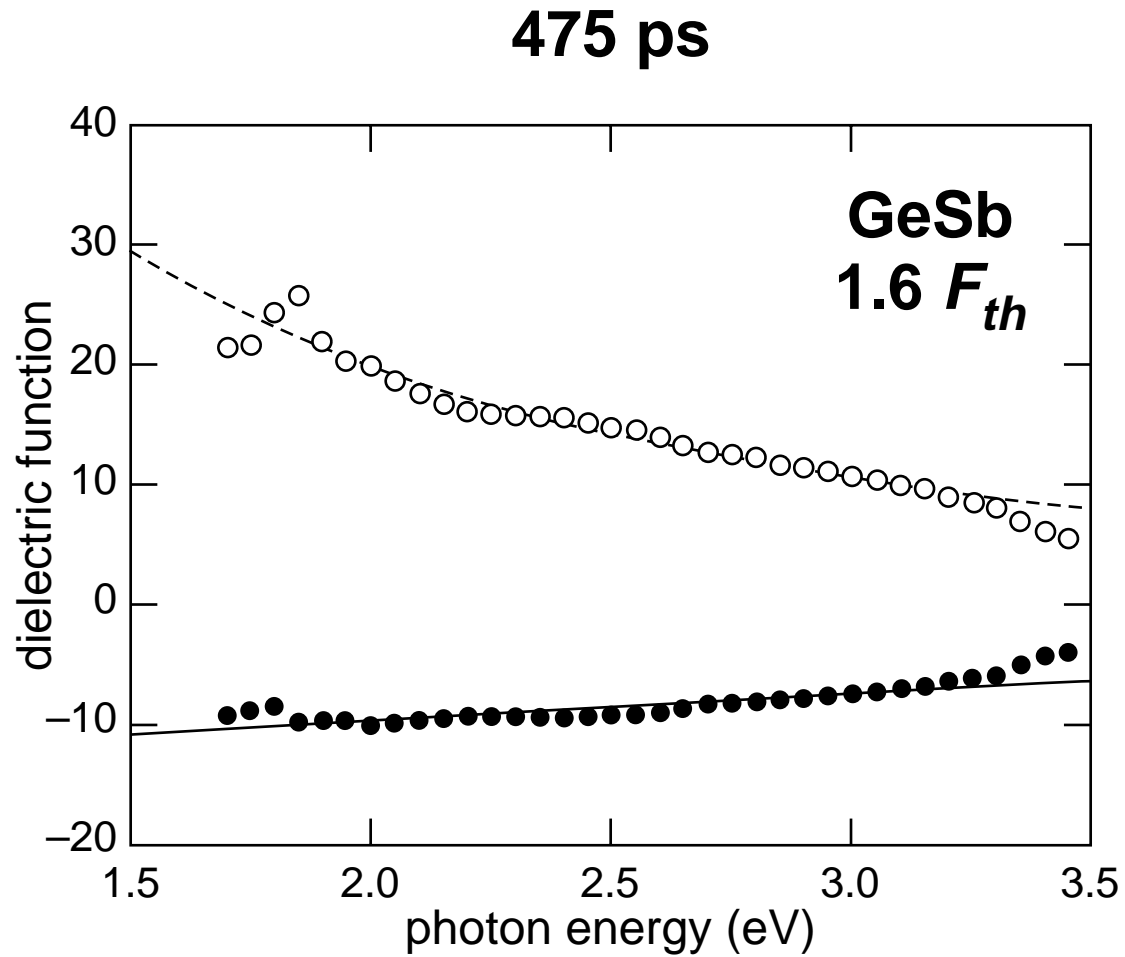
not crystalline

Results



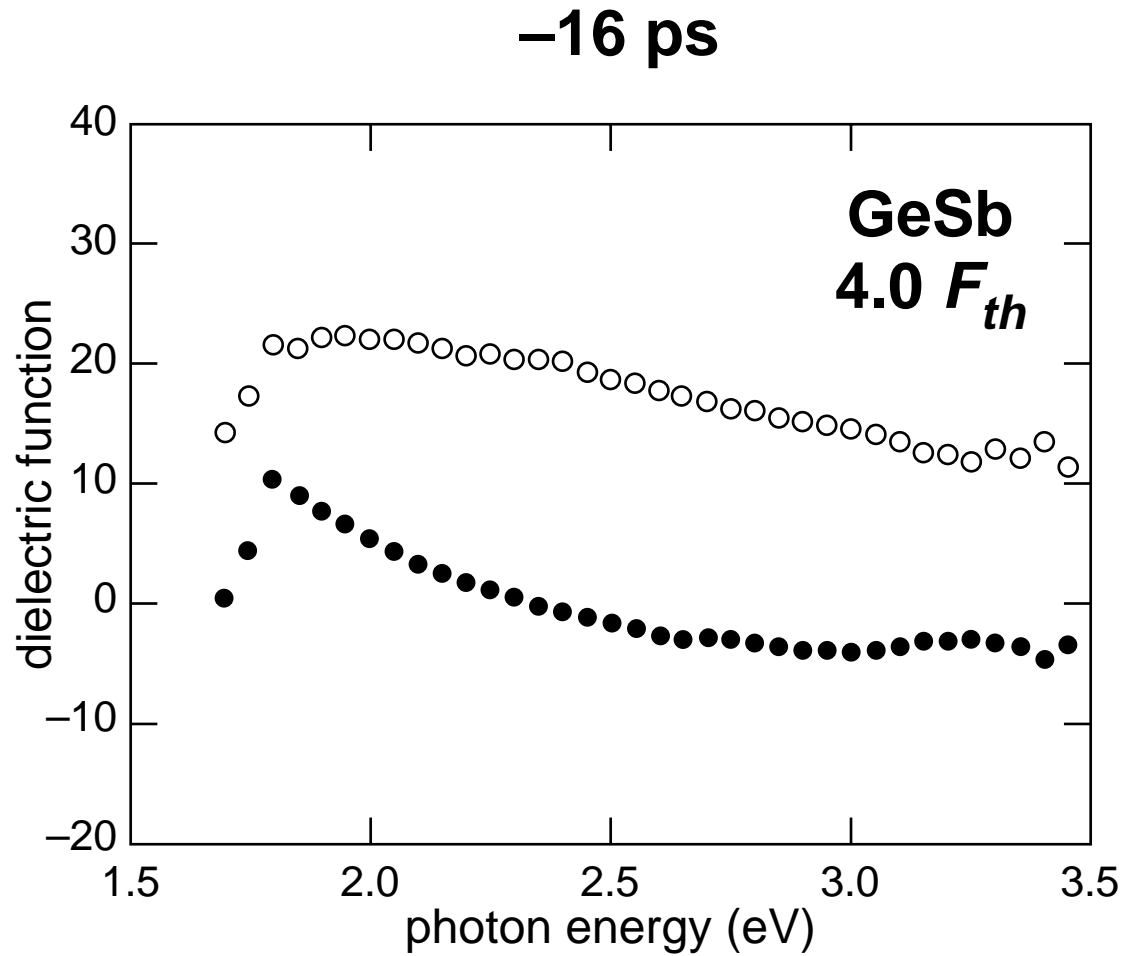
not crystalline

Results



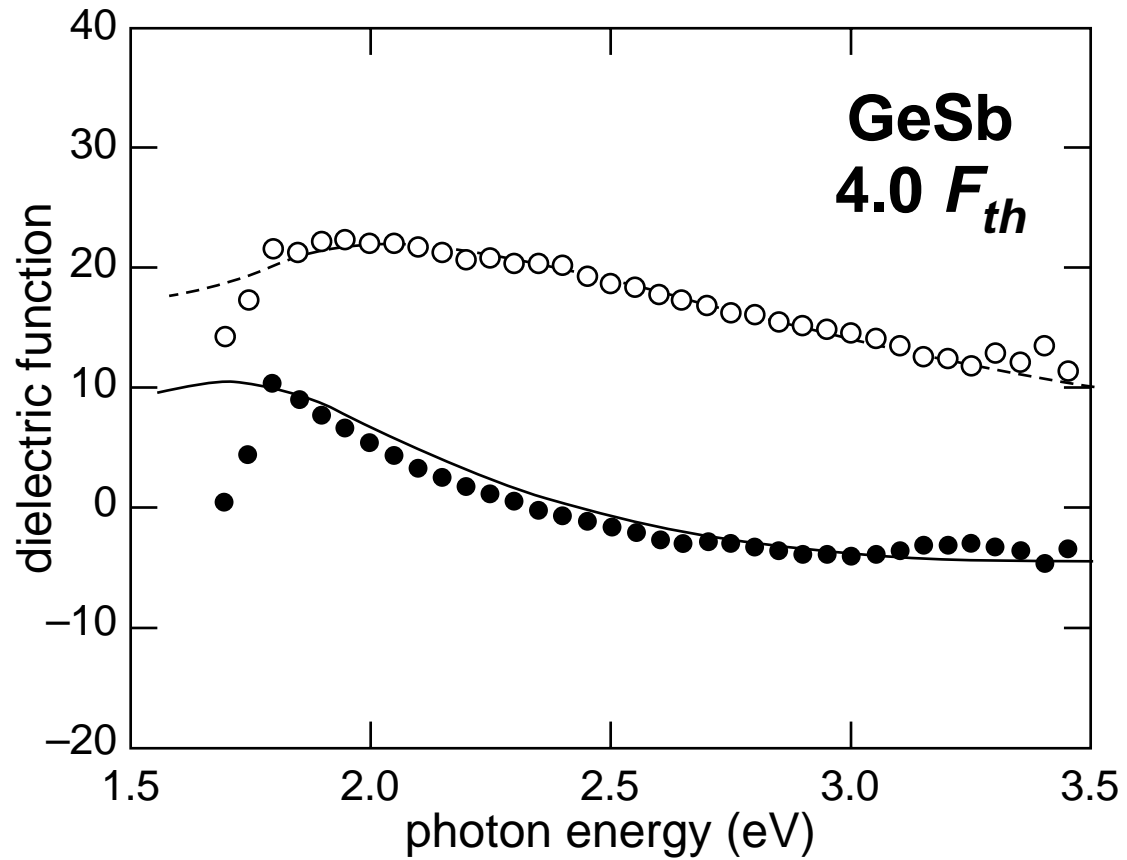
Drude-like after 1 ps

Results

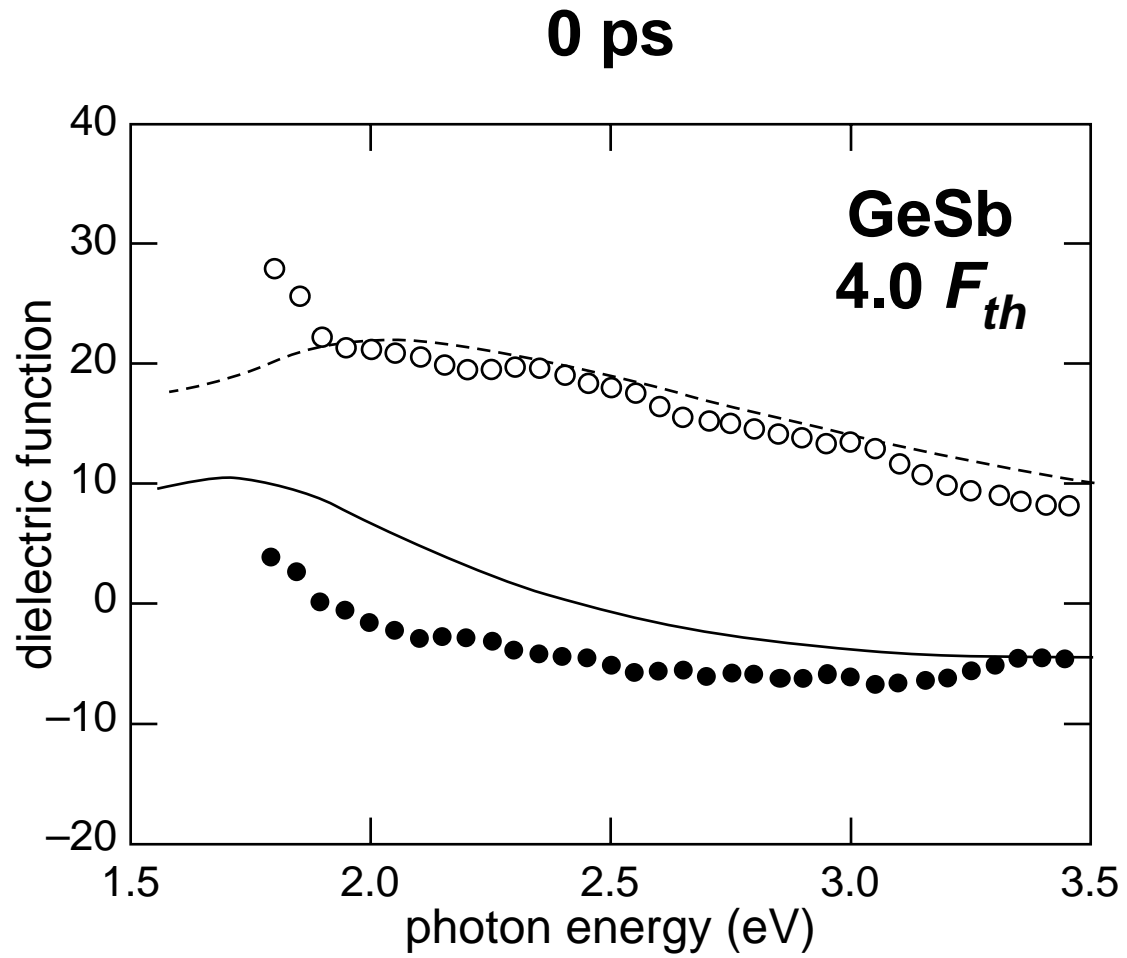


Results

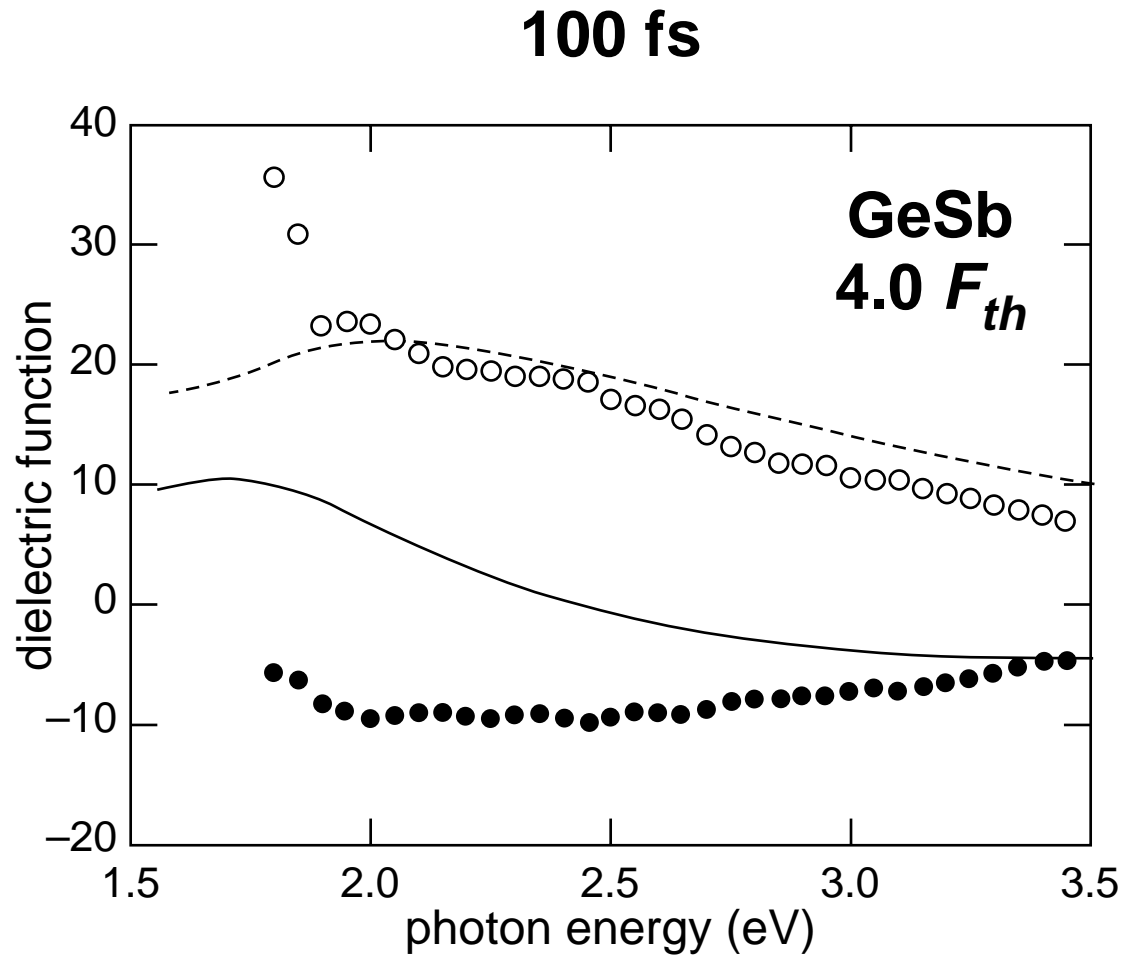
-16 ps



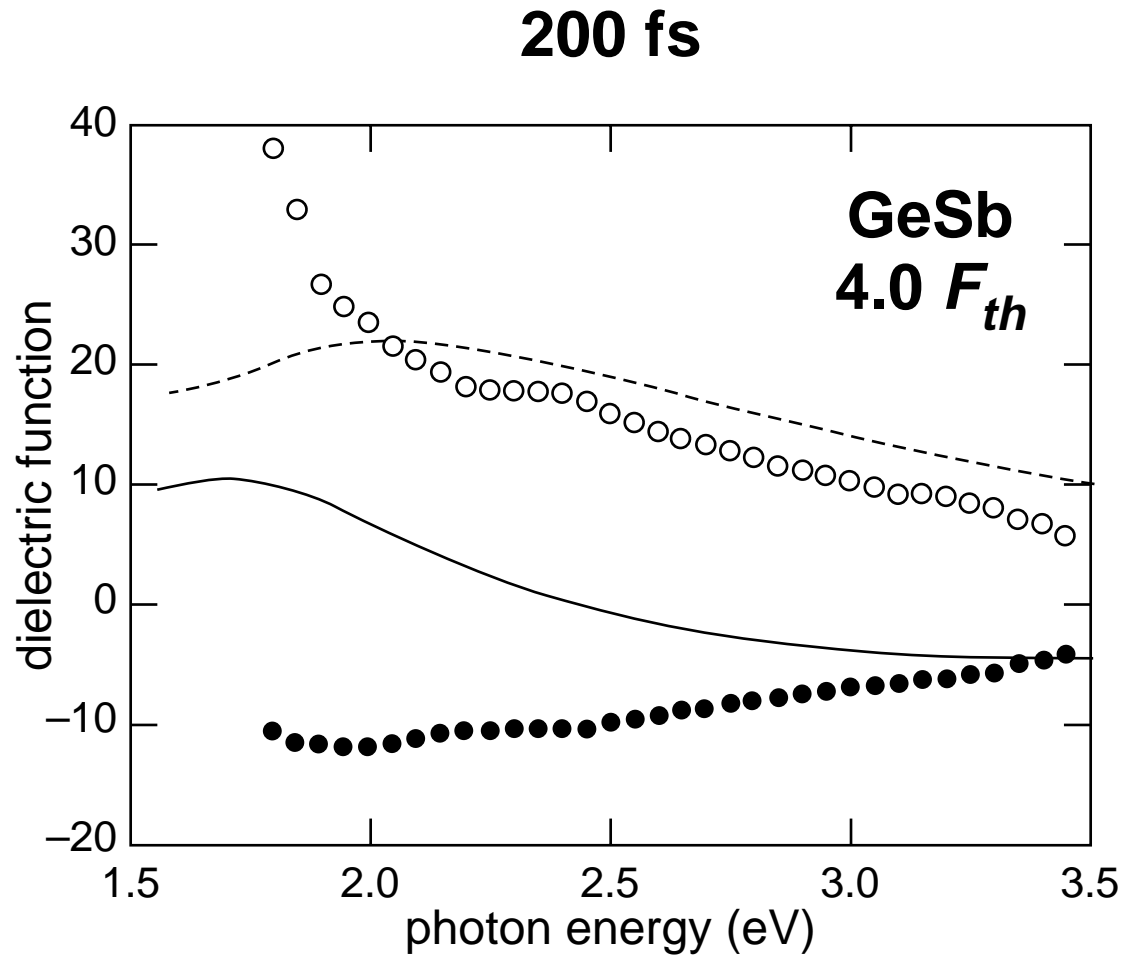
Results



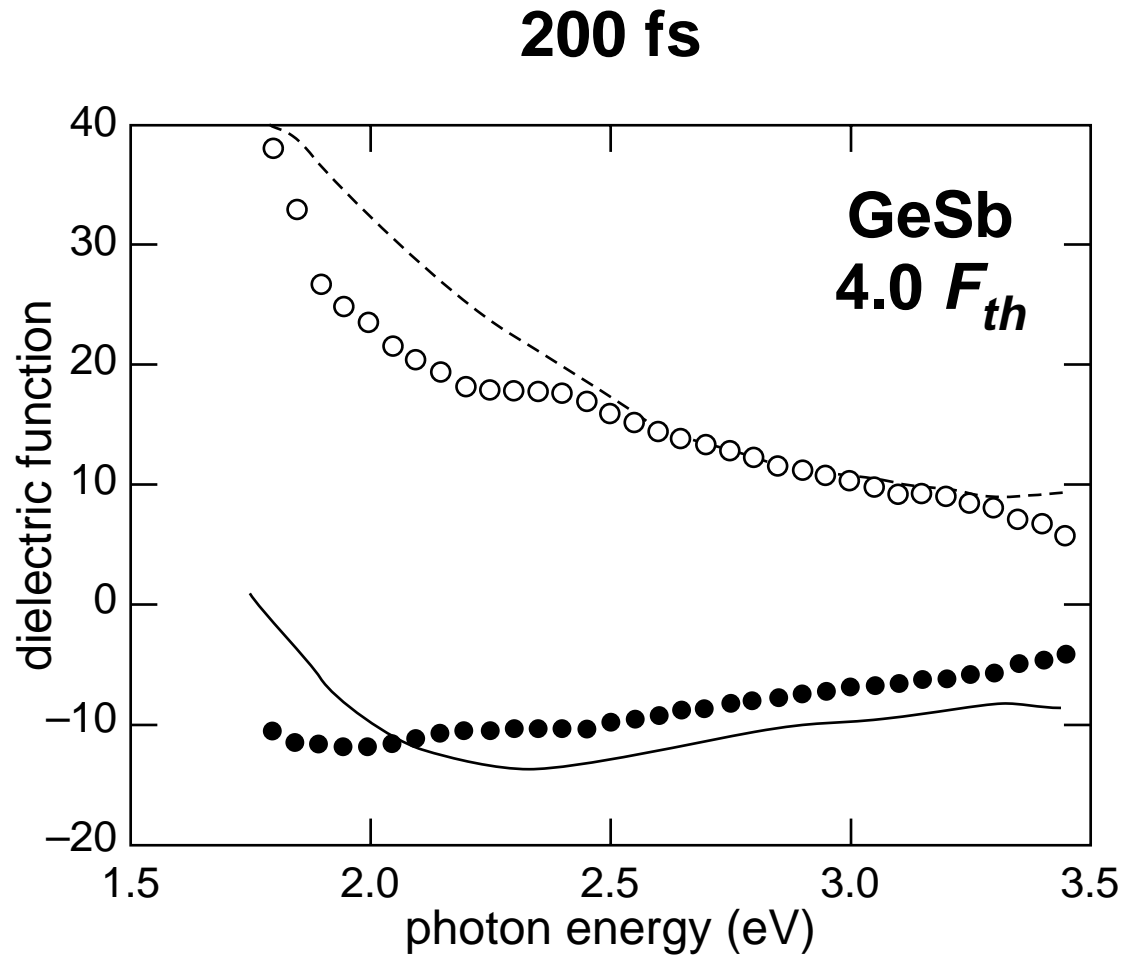
Results



Results

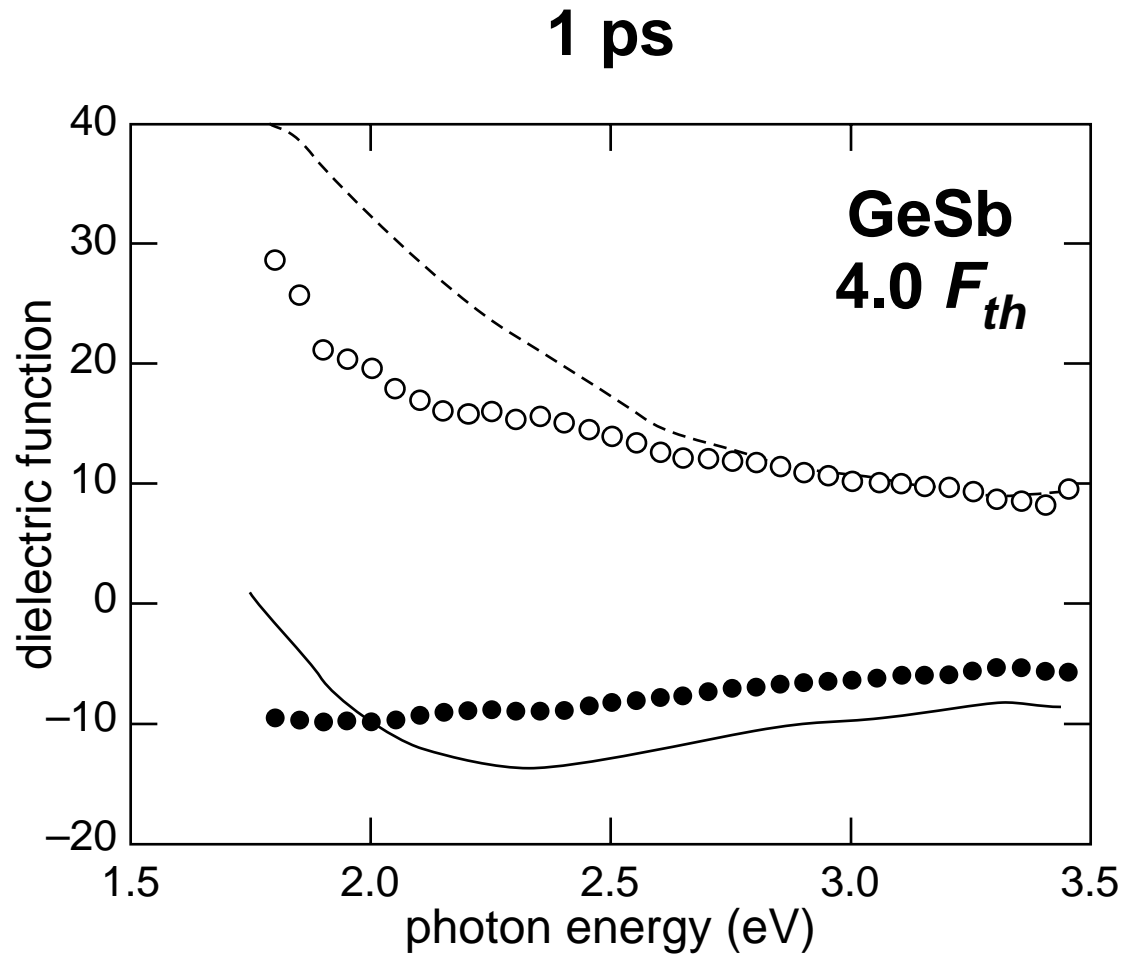


Results



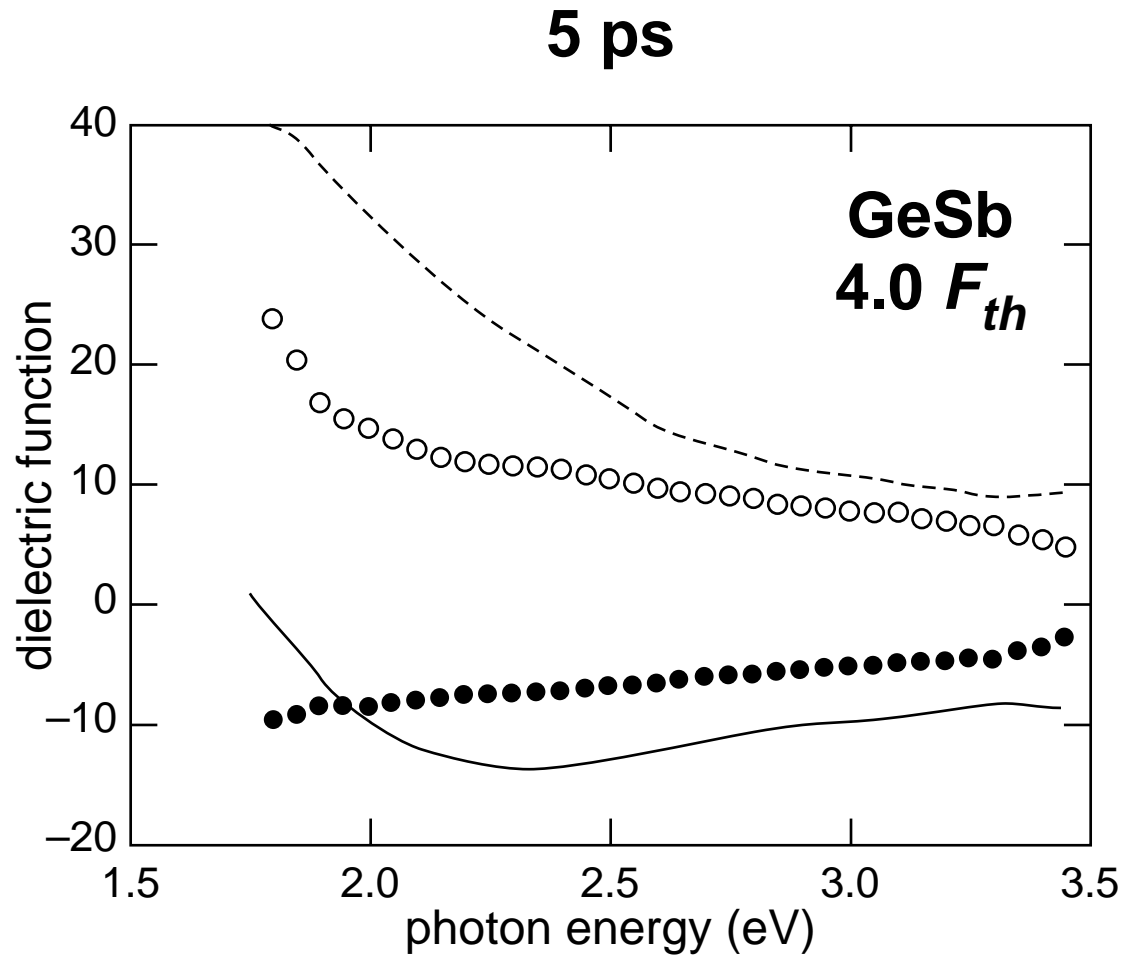
more Drude-like than crystalline

Results



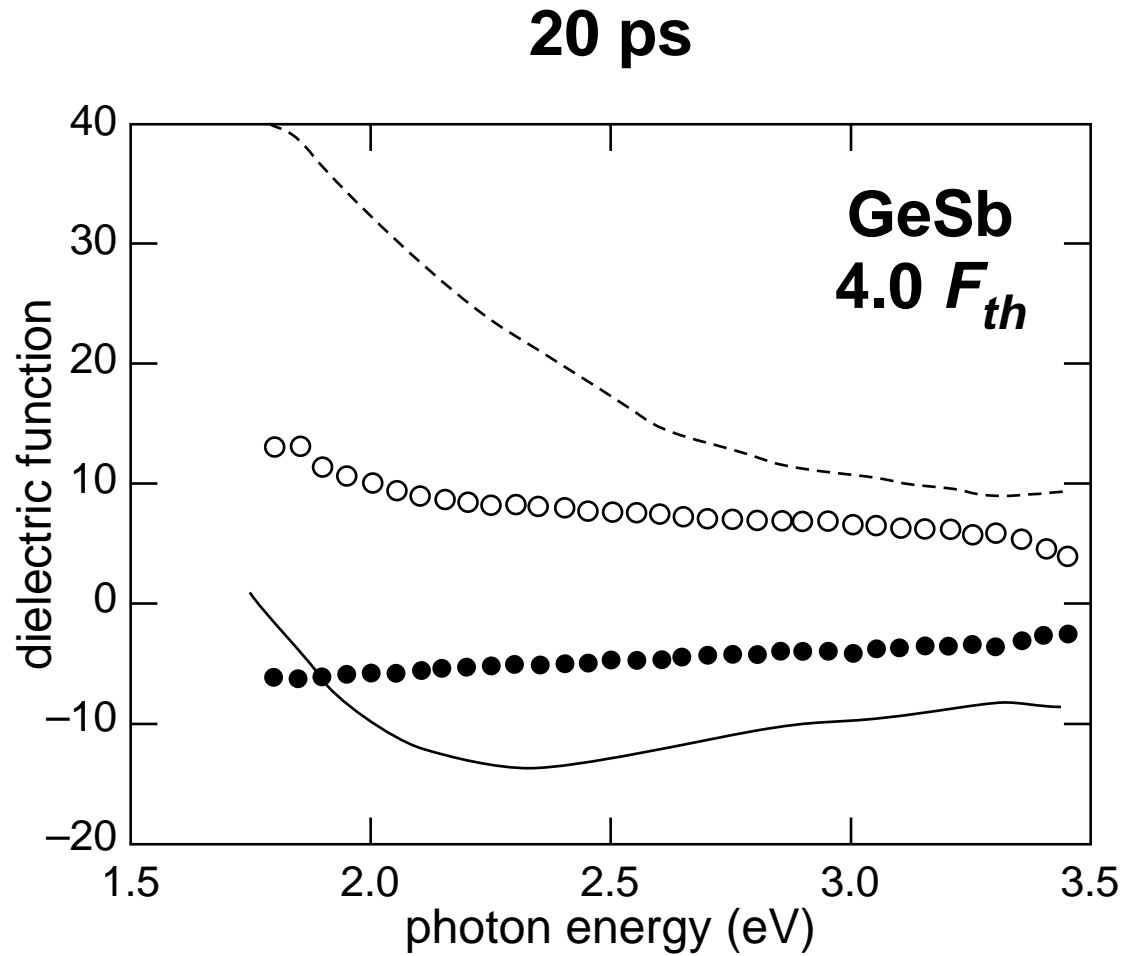
more Drude-like than crystalline

Results



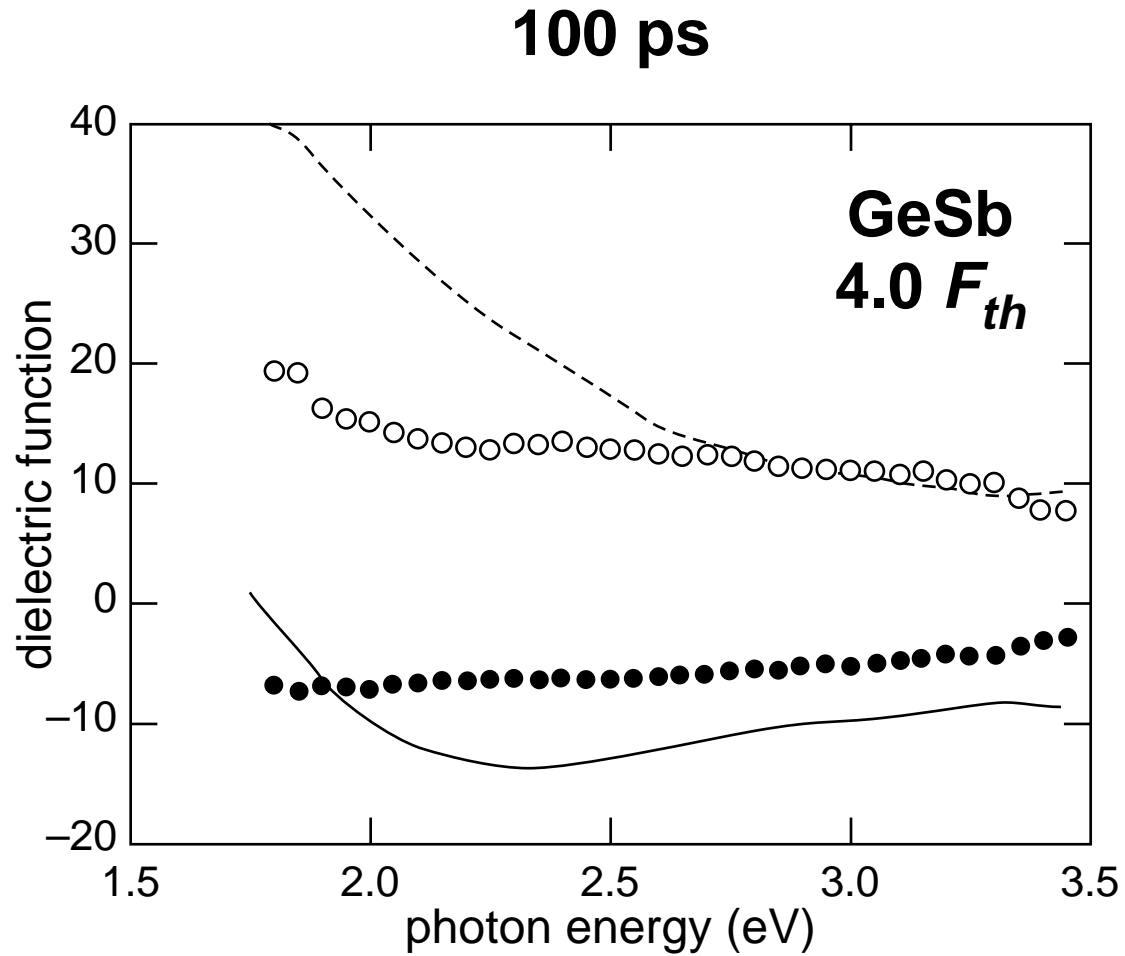
more Drude-like than crystalline

Results

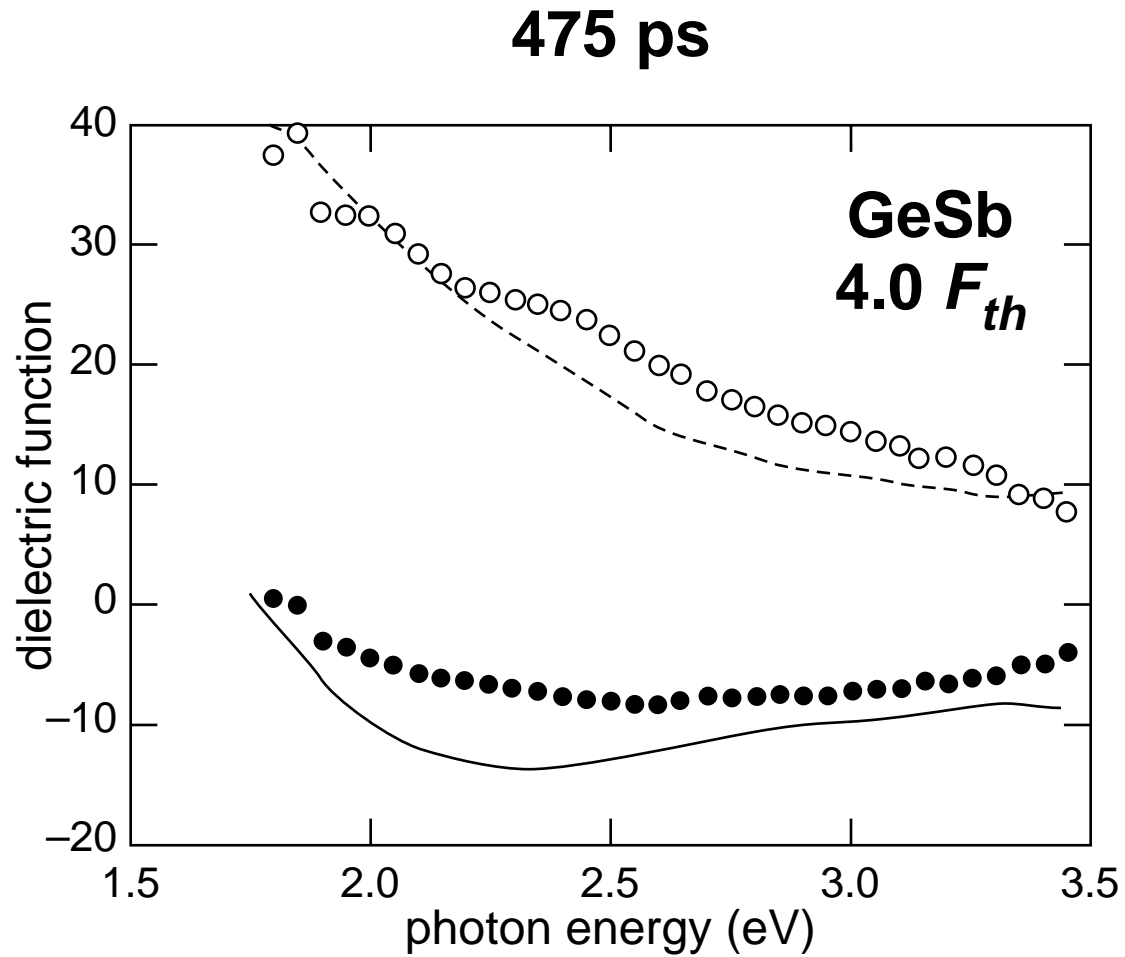


more Drude-like than crystalline

Results



Results



recrystallization

Summary

- ▶ **recrystallization in less than a nanosecond**
- ▶ **intermediate phase metallic, but not crystalline**
- ▶ **data provide wealth of additional information**

Summary

Femtosecond time-resolved ellipsometry

- ▶ **powerful tool for tracking ultrafast electron and lattice dynamics in highly excited solids**
- ▶ **helps uncover unexplored terrain on the boundary between condensed matter and plasma physics**

GORDON MCKAY
LABORATORY OF
APPLIED SCIENCE



Funding: National Science Foundation

Acknowledgments:

Prof. Dietrich von der Linde

Dr. Klaus Sokolowski-Tinten

Dr. Craig Arnold

**For a copy of this talk and
additional information, see:**

<http://mazur-www.harvard.edu>

